culture dish, without apparent apoptosis. SV40 large T antigen overcomes normal senescent pathway by inactivating some proteins, which are associated with cell proliferation, such as tumor suppressor gene p53 and pRB proteins. Interestingly, 6-16 is still expressed in SV40-transformed cells after extending their life-span [6]. 6-16 expression may be independent from p53 pathway and/or pRB pathway. Interestingly, we found that human senescent fibroblasts express 6-16 by producing interferon-β by autocrine mechanism. Interferon regulatory factor 1, IRF-1, is a major regulator of the interferon signaling pathway. Treatment of anti-IRF-1 antibody to human senescent cells or life-extended SV40-transformed fibroblasts resulted in down-regulation of 6-16 expression [6]. It is still unknown how senescent cells are protected from apoptosis, because senescent cells could be attached to the dish and are viable for more than 1 year with just a medium change; hence, it is believed that some anti-apoptotic gene may be protecting the senescent cells from apoptosis.

Attenuation of apoptosis appears recession for establishment and maintenance of transformed phenotype [7]. We found that 6-16 gene is expressed at a high level in immortalized cells and in gastrointestinal tumor cells. These data suggest that an increase in expression of 6-16 is associated with attenuation of apoptosis.

Mitochondria is an important organelle for the control of apoptosis, in addition to the role as the center of energy metabolism, and influence the commitment of cell death by regulating the mitochondrial permeability and membrane potential [8–11]. Bcl-2, an anti-apoptotic protein, is known to be located on mitochondria and expressed at high level in some tumor cells and tissues [11]. We report here that 6-16 is relatively expressed in cancer cells and tissues, and 6-16 is a novel anti-apoptotic protein located in the mitochondria and can be a new target for cancer chemotherapy and mitochondrial diseases.

Materials and methods

Northern blotting and RT-PCR

RNA isolation and Northern blotting were performed as described previously [6]. All 6-16 splice valiants are recognized by the probe for Northern analysis. RT-PCR was performed according to the protocol with the Thermoscript one-step RT-PCR system (Invitrogen, USA). For the detection of B and C type of 6-16 spliced valiants, we used 5′-GGGTGGAGGCAGGTGAGAATGCGG-3′ as the forward primer and 5′-TGACCTTCATGGCCGTCGGAGGAG-3′ as the reverse primer. Samples were incubated at 50°C for 30 min and denatured at 94°C for 2 min, and then cycled 32 times with 30 s at 94°C and 30 s at 62°C followed by a final extension step of 5 min at 68°C. GAPDH was used for internal control for validating RNA amounts as described before [12].

In situ mRNA hybridization analysis

In situ mRNA hybridization (ISH) was performed as described previously [13] with minor modification. Briefly, an interferon inducible gene 6-16-specific oligonucleotide probe was designed complementary to the 5′-end of human 6-16 mRNA transcript (GenBank NM022873). The DNA oligonucleotide sequence 5′-CGCCGCCCCCATTCAGGA-3′ was of the antisense orientation and hence complementary to 6-16 mRNA. To verify the integrity and lack of degradation of mRNA in each sample, we used a d(T) oligonucleotide. All DNA probes were synthesized with six biotin molecules (hyperbiotinylated) at the 3′-end via direct coupling using standard phosphoramidite chemistry (Research Genetics, Huntsville). ISH was carried out using the Microprobe manual staining system (Fisher Scientific, Pittsburgh). A positive reaction in this assay stained red. Control for endogenous alkaline phosphatase included treatment of sample in the absence of the biotinylated probe and use of chromogen alone. To check the specificity of the hybridization signal, the following controls were used: RNAse pretreatment of tissue sections, substitution of the antisense probe with a biotin-labeled sense probe, and competition assay with unlabeled antisense probes. No or markedly decreased signals were obtained after either of these treatments.

Antibody

Rabbit polyclonal antibody against human 6-16 was raised against synthetic peptide (YATHKYLDSEEDEE) corresponding to amino acid residues 117–130 of human 6-16, and was purified by MAbTrap GII affinity chromatography kit (Amersham Bioscience, USA). This antibody was sufficient for immunoblotting but insufficient for immunoprecipitation and immunostaining of 6-16 protein. Another rabbit polyclonal anti-human 6-16 antibody (OT904-1A) was also prepared against synthesis peptides (VEAGKKKCSESSDSG) corresponding to amino acid residues 21–35 of human 6-16. This antibody was sufficient for immunostaining. Mouse monoclonal anti-human CIB antibody was kindly provided by Leslie V. Parise. Anti-cytochrome c antibody (clone 7H8.2C12 which recognizes the denatured form of human, mouse and rat cytochrome c; BD Pharmingen, USA), monoclonal anti-human Bcl-2 antibody (clone124, Upstate Biotechnology, USA) and polyclonal anti-Bax antibody (Upstate Biotechnology) were used for immunoblot and immunoprecipitation. Anti-cytochrome c antibody (clone 6H2.B4 which recognizes the native form of human, mouse and rat cytochrome c; BD Pharmingen) was used for immunostaining. Polyclonal anti-GST rabbit antibody (New England Biolabs, USA) and polyclonal anti-MBP antibody (kindly provided by Dr. M. Nakata, Sumitomo Electric Industries, Japan) were used for immunoblot.

Cell culture, PI staining, caspase-3 activity assay, and mitochondrial membrane potential assay

The 0.8 kb fragment encoding full length 6-16 was inserted in the pCXN vector, which was digested with Xho I and blunted with klenow fragment. To establish stable transfected TMK-1 cells expressing 6-16 (TMK-1-6-16), TMK-1 cells were transfected with pCXN/6-16 vector and were selected for neomycin resistance with 200 μg/ml Geneticin (Invitrogen, USA). Gastric cancer cell lines, TMK-1, TMK-1-6-16 and MKN-28 were cultured at 37°C and 5% CO_2 in RPMI 1640 (Invitrogen) supplemented with 10% FCS and Antibiotic-Antimycotic (Invitrogen). A normal human fetal fibroblast strain, TIG-3, was cultured in Dulbecco's modified Eagle medium (Invitrogen) supplemented with 10% FCS and Antibiotic-Antimycotic (Invitrogen).

Apoptosis was induced by actinomycin D (10, 20 and 40 μg/ml) for 24 h, cycloheximide (10, 30 and 100 μM) for 6 h, H_2O_2 (0.5, 5 and 50 μM) for 6 h, etoposide (200, 400 and 600 μM) for 24 h, bleomycin (100, 200 and 400 μg/ml) for 24 h, 5-FU (100, 200 and 400 μg/ml) for 24 h, aphidicolin (100, 200 and 400 μM) for 24 h or serum-deprivation for 60 h. Cells were collected and stained with PI-RNase solution (BD Biosciences, USA), and were analyzed for DNA content by Flow cytometry on a FACS Calibur. For DNA ladder analysis, apoptotic DNA was extracted by lysis buffer (50 mM Tris-HCl pH7.5/ 20 mM EDTA/1% NP40), and run on 2% agarose gel.

For Caspase-3 activity analysis, cells were grown in six-well plates overnight, and were treated with CHX (10 and 30 μM) for 6 h or with 5-FU (80 μg/ml) for 24 h. Cells were collected and incubated with PhiPhiLux substrate buffer (OncoImmunin Inc., Gaithersbury, MD, USA) for 60 min at 37°C in 5% CO_2 incubator, and were analyzed by Flow cytometry on a FACS Calibur.

For mitochondrial membrane potential analysis, cells were grown in six well plate overnight, and were treated with CHX (10 and 30 μM) or 5-FU (50 and 100 μg/ml) for an hour. Cells were collected and incubated with Mitosensor reagent buffer (Clontech) for 30 min at 37°C in CO_2 incubator, and were analysis by Flow cytometry on a FACS Calibur.

Immunofluorescence analysis

Cells grown on eight-well Lab-Tek chamber slides (Nalge Nunc International, Napaperville, IL) were fixed in 4% paraformaldehyde / PBS (pH 7.4) for 20 min and permeabilized in blocking buffer (0.2% Triton X-100/ 3% BSA/PBS) for 30 min. The cells were incubated for 1 h at room temperature with mouse anti cytochrome c monoclonal antibody (6H2.B4) diluted 1:100, or with rabbit anti-human 6-16 polyclonal antibody (OT904-1A) diluted 1:100 in blocking buffer. The cells were washed four times in PBS and incubated with Alexa FluorTM 488 goat anti-mouse IgG conjugate (Molecular Probes, USA) or with Alexa FluorTM 488 goat anti-rabbit IgG conjugate (Molecular Probes) diluted 1:200 in blocking buffer for an hour at room temperature. Immunofluorescent staining was analyzed using a confocal laser-scanning microscope (LSM510, Carl Zeiss, Germany).

Mitochondria were labeled in intact cells with Mito-Tracker CM-H_2XRos (Molecular Probes). Cells were incubated in the MitoTracker medium (final concentration 500 nM) for 45 min before finishing to treat with CHX or 5-FU. Then, the cells were fixed, permeabilized and double-labeled with anti-cytochrome c antibody (6H2.B4) as described above.

Cell fractionation, immunoprecipitation and immunoblot analysis

For isolation of cellular fraction, cells were suspended in sucrose-supplemented extraction buffer (SCEB, 300 mM sucrose, 10 mM HEPES pH 7.4, 50 mM KCl, 5 mM EGTA, 5 mM $MgCl_2$, 1 mM DTT, protease cocktail), left on ice for 30 min, and homogenized by 70 strokes in an ice-cold Dounce homogenizer. Unbroken cells and nuclei were pelleted by centrifugation for 10 min at 2,000×*g*, and the supernatant was further spun at 13,000×*g* for 20 min to separate mitochondria-rich fraction from cytosol fraction. The pellet was resuspended in 50 μl of SCEB (mitochondria fraction), and the supernatant was cytosolic fraction.

For co-immunoprecipitation experiments, cells were lysed in NP-40 lysis buffer (50 mM Tris-HCl, pH7.4, 120 mM NaCl, 1% NP-40) containing protease inhibitor cocktail (Roche, USA). Antigen-antibody reaction was performed by incubating 0.5 ml (500 μg protein) of the cell extract with rabbit anti-human 6-16 antibody (117–130), mouse anti-CIB antibody, rabbit anti-Bax antibody or mouse anti-Bcl-2 antibody overnight at 4°C. The immunocomplex were incubated with 50 μl protein-G-Sepharose for 3 h at 4°C, and the beads were washed three times with NP-40 lysis buffer and boiled in Laemmli buffer.

For immunoblot analysis, the proteins were separated on 13% or 15% SDS-PAGE, and transferred to Immobilon-P (Millipore) and immunoblotted with anti-6-16 antibody (117–130), anti-CIB antibody, anti-Bcl-2 antibody, anti-Bax antibody or anti-cytochrome c antibody (7H8.2C12) diluted 1:500. The signal was detected using ECL-Plus (Amersham Bioscience).

Yeast two-hybrid assay

Dr Y. Takai (Osaka University, Suita, Japan) kindly supplied yeast L-40 strain and pBTM116/HA for yeast two-hybrid screening. A strain of L40 carrying pBTM116/6-16 was transformed with pGADGH HeLa cDNA library (Clontech). Approximately 1×10^6 transformants were screened for the growth on SD medium

plated lacking Trp, Leu, and His as evidenced by transactivation of a LexA-HIS3 reporter gene and His prototrophy. His+ colonies were scored for β-galactosidase activity. Plasmids harboring cDNAs were recovered from positive colonies and introduced by electroporation into *E. coli* HB101 on the M9 plate lacking Leu. Then the plasmids were recovered from HB101 and transformed again into L40 containing pBTM116HA/6-16. The nucleotide sequences of plasmid DNAs were determined.

Interaction of proteins in vitro

6-16-pGEX-2T (Amersham Bioscience) or CIB-pMAL-C2 (New England Biolabs) expression vectors were constructed to produce GST-6-16 and MBP-CIB proteins. GST-6-16 and MBP-CIB proteins were purified from *E. coli* transformed with their expression vectors treated with 0.1 M IPTG by using amylose resin (New England Biolabs) or glutatione Sepharose 4B (Amersham Bioscience). GST-6-16 protein (20 pmol) was incubated with MBP-CIB protein (40 pmol) in 40 μl of reaction buffer (20 mM Tris-HCl pH7.5, 1 mM DTT and 0.05% CHAPS) for 1 h at 4°C. After glutathione Sepharose 4B (Amersham Bioscience) was added and further incubated for 1 h, the precipitates were washed three times and subjected to immunoblot analysis using anti-MBP and anti-GST rabbit polyclonal antibody.

Results

6-16 was expressed in gastric cancer cells and tissues

We examined expression levels of 6-16 mRNA in eight gastric cancer cell lines (MKN-1, MKN-7, MKN-28, MKN-45, MKN-74, TMK-1, HSC-39 and KATO III) by Northern blot analysis. Seven out of eight gastric

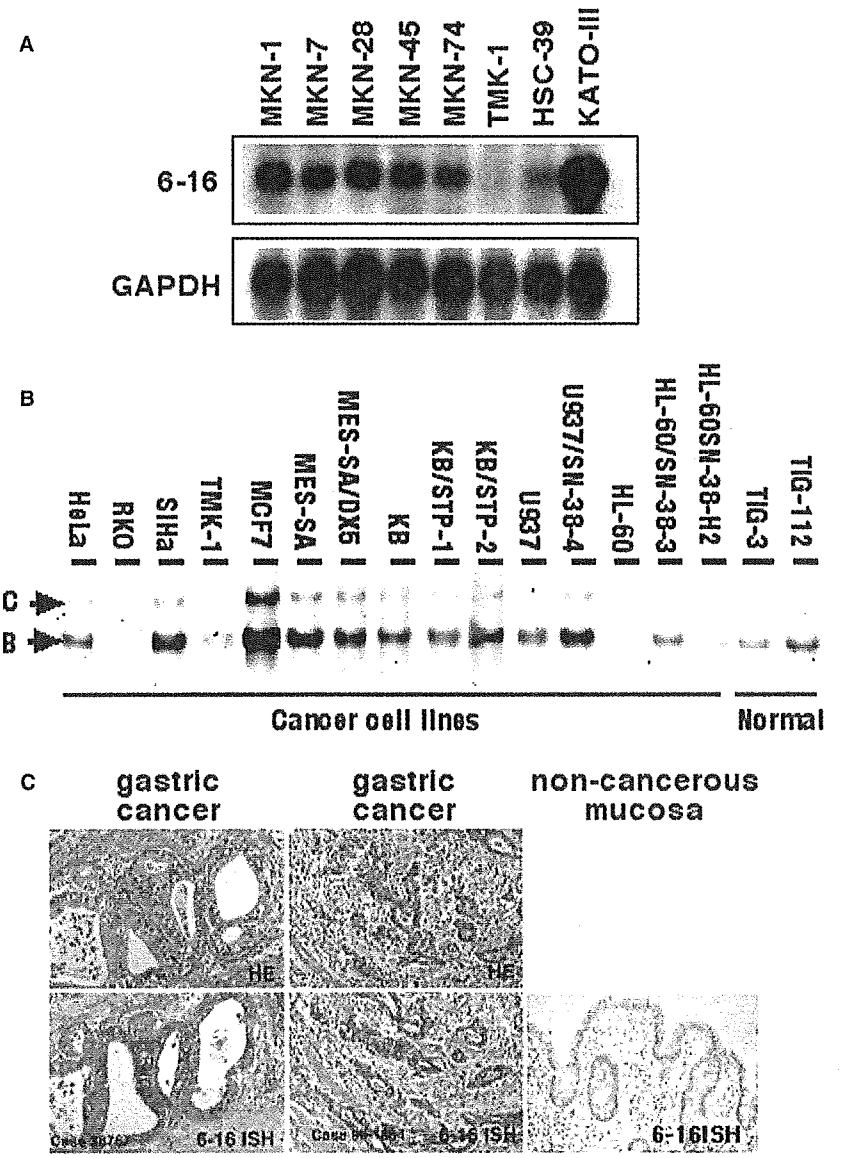

Fig. 1 Expression of 6-16 mRNA in gastric cancer cells and carcinoma tissues. **a** Expression of 6-16 mRNA was detected by Northern blot analysis with 10 μg total RNA in eight gastric cancer cell lines. Hybridization of a G3PDH (control) probe to the same filter membrane is depicted in the *lower panel*. **b** Expression of 6-16 mRNA was detected by RT-PCR analysis. 0.2 μg of RNA were used for RT-PCR reaction. PCR products were run on 6% acrylamide gel electrophoresis and staining with CYBR Green I nucleic acid staining. **c** Surgically resected adenocarcinomas of the stomach were examined on in situ hybridization using the microprobe manual staining system (Fisher Scientific). 6-16-specific anti-sense oligonucleotide DNA probe (5′-GCA CGC CGC CCC CAT TCA GGA TCG CAG-3′) was designed. *lower panel* 6-16 in situ hybridization. *upper panel* hematoxylin-eosin (HE) staining

carcinoma cell lines expressed 6-16 mRNA, while TMK-1 cells showed very low levels (Fig. 1a). p53 mutation (codon 173, GTG to ATG) was found in TMK-1 cells [14]. Other gastric cell lines also have p53 mutation excluding MKN-45 [14]. However, there is no correlation between p53 mutation status and 6-16 expression levels. TMK-1 cell is sensitive to apoptosis compared with other gastric cancer cell line used in Fig. 1a. In the other cancer cell lines that were frequently used for apoptosis research, colorectal cancer cell line RKO, which is sensitive to apoptosis, express low levels of 6-16. In contrast, high levels of 6-16 expression was found in breast cancer cell line MCF-7 cell, which is resistant to apoptosis (Fig. 1b). Interestingly, HL-60 cell line does not have a significant level of 6-16 expression, but anti-cancer drug resistant clone of HL-60 cells do have high levels of 6-16 expression (Fig. 1b). Human uterine sarcoma cell line, NES-SA and the multiple drug-resistant uterine sarcoma cell line, MES-SA/DX7 also express high levels of 6-16, but there is significant difference between these two cell lines. Taken together, there is good correlation between 6-16 expression levels and resistant to apoptosis. We next studied the expression of 6-16 mRNA in primary gastric carcinomas by in situ mRNA hybridization (ISH) (Fig. 1c). In almost all of these tumors, higher expression of 6-16 mRNA was shown in cytoplasm of the tumor cells in comparison with the corresponding non-neoplastic mucosas. We also recognized weak signal in stromal fibroblast cells and fundic gland cells, but not in muscular tissues of the gastrointestinal tracts (Fig. 1c).

6-16 is 32 kDa glycosylated protein

To elucidate the function of 6-16, we established 6-16 expressing TMK-1 cells by transfection of 6-16 cDNA. After selection with G418, we isolated several clones and examined the expression of 6-16. Among them, clone 8 expresses the highest level of 6-16 mRNA (Fig. 2a). Isolated clones in order of 6-16 expression levels are No. 8, 11 and 3. Clone 11 also expresses 6-16, but slightly lower than clone 8. Expression of 6-16 in clone 3 is lowest in these clones. We used these three types of clones to examine the function of 6-16. Unless otherwise indicated, TMK-1-6-16 clone 8 is referred to as TMK-1-6-16, and is used for further examination in comparison with the parental TMK-1.

To analyze 6-16 protein expression, we generated 6-16 polyclonal antibody that was raised against synthetic peptide (YATHKYLDSEEDEE) corresponding to amino acid residues 117–130 of human 6-16 and was purified by MAbTrap GII affinity chromatography. Theoretical molecular weight of 6-16 is about 14 kDa protein by using ExPASy molecular biology database server. By using in vitro transcription/translation

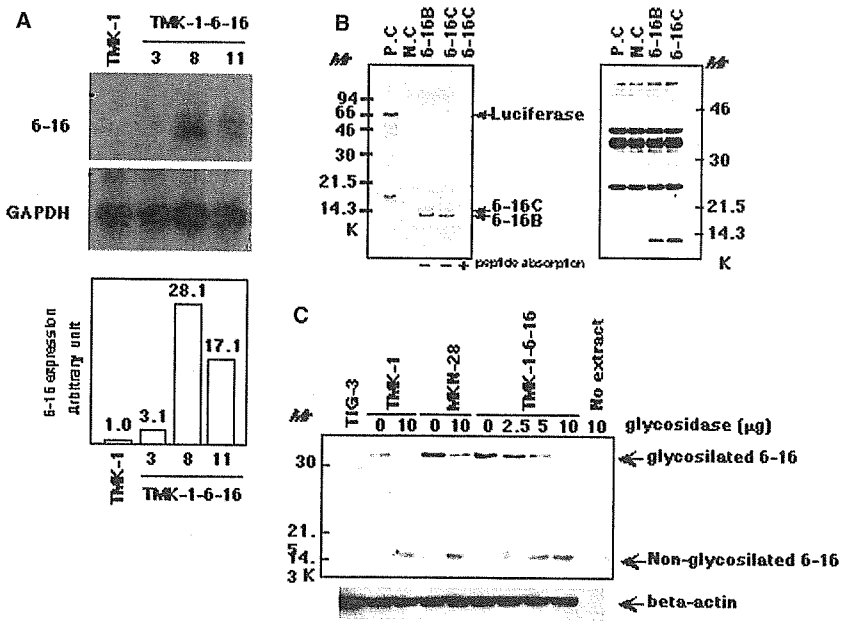

Fig. 2 Localization of 6-16 at mitochondria. **a** Total RNA was isolated from each cell line, and 10 μg of each was used for Northern blot analysis. Semi-quantitative analysis of 6-16 mRNA level of autoradiographs was performed using the public domain NIH Image program. The units are arbitrary, and were calculated based on the expression of 6-16 mRNA in TMK-1 cells as 1.0. Hybridization of a G3PDH (control) probe to the same filter membrane is depicted in the *lower panel*. **b** In vitro transcription/translation products were synthesized from luciferase control (positive control: P.C), pZero/Kan (negative control: N.C) and 6-16-pZero/Kan expression vector by using TNT coupled Wheat Germ Extract System (Promega). Incorporation products of ^{35}S-methionine were detected by autoradiography after separating by 15% SDS-PAGE (*left panel*). Non-radioactive products were detected by immunoblot analysis with anti-6-16 antibody (*right panel*). C, Extracts from TIG-3, TMK-1, TMK-1-6-16 and MKN-28 cells were incubated with different concentrations of glycosidase at 37°C for 48 h, and detected by immunoblot analysis with anti-6-16 antibody

experiments from 6-16 cDNA, 14 kDa protein was detected both by autoradiography of ^{35}S-methionine-incorporated products and immunoblotting using a specific antibody (data not shown). By using cell extract from human culture cell, we could not detect 14 kDa 6-16 protein by Western blotting analysis, but 32 kDa protein was detected in 6-16 highly expressing cells such as TMK-1-6-16 and MKN-28. TIG-3 and TMK-1 cells are low or no 6-16 expression by immunoblotting analysis (Fig. 2b). Thus, it is speculated that 6-16 has some protein modifications such as phosphorylation or glycosilation. By the ProDom database analysis (motif), 6-16 protein has multiple possible glycosylation sites including 15 serine residues and 5 threonine residues. To clarify this possibility that 6-16 protein is glycosilated, we treated glycosidase to the cell lysates that were isolated from TMK-1 and TNK-1-6-16 cells, and performed SDS-PAGE and immunoblotting. By digestion with glycosidase, the shift of 32 kDa protein band to 14 kDa band was observed with increasing enzyme concentration, indicating an extensive glycosylation of the native 6-16 protein (32 kDa) in cells (Fig. 2b). These results suggest that 6-16 protein is 34 kDa glycosilated protein.

Apoptosis was attenuated in cells expressing 6-16 protein at high level

6-16 protein is expressed at high levels in both tumor cells and senescent cells. As shown in Fig.1, most of the gastric cancer cell lines expressed 6-16 at high levels except TMK-1 cell. So, we examined whether overexpression of 6-16 protein has an effect on the apoptosis. Out of eight inducers of apoptosis field such as actinomycin D, cycloheximide (CHX), H_2O_2, etoposide, bleomycin, 5-fluoro-2′-deoxyuridine(5-FU), aphidicolin or serum-deprivation, only CHX, 5-FU and serum-deprivation induced apoptosis in TMK-1. However, in TMK-1-6-16 cells which are overexpressing 6-16 protein, apoptosis induced by CHX or 5-FU were significantly inhibited by subG0 analysis using Flow cytometry (Fig. 3a). The other five inducers of apoptosis did not induce apoptosis in either TMK-1 and TMK-1-6-16 cells (data not shown). The increase in subG0 fraction was observed in the dose-dependent manner after CHX or 5-FU treatment in TMK-1, but not in TMK-1-6-16 cells (Fig. 3a). TMK-1-6-16 (clone 3) and TMK-1-6-16 (clone 11) expressed less 6-16 (Fig. 1b) and was less resistant to CHX or 5-FU induced apoptosis than TMK-1-6-16

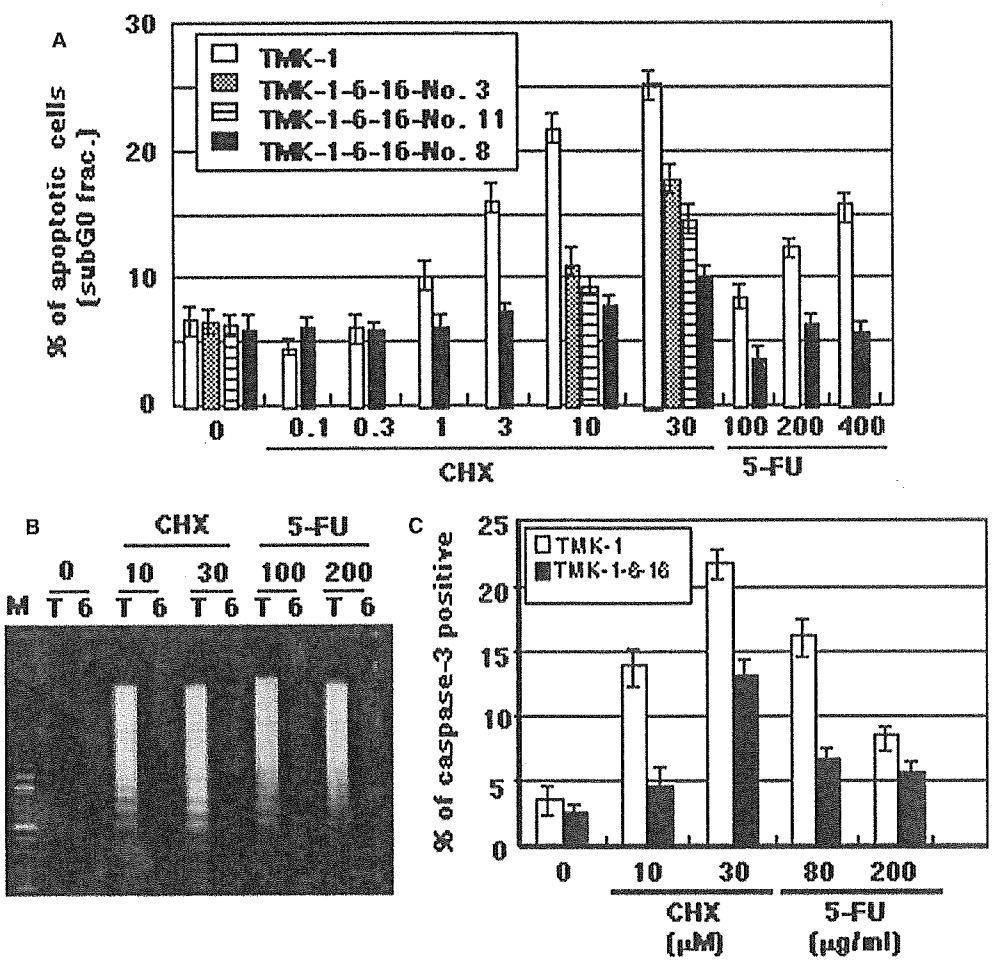

Fig. 3 6-16 inhibits apoptosis and caspase-3 activity by CHX and 5-FU. **a** TMK-1 and TMK-1-6-16 cells were treated with CHX for 6 h or with 5-FU for 24 h. Cells were collected and stained with PI-RNase solution, and were analyzed for DNA content by Flow cytometry. Percentage of cells with subG0 DNA content was calculated. **b** TMK-1 (T) and TMK1-6-16 (6) cells were treated with CHX (10 and 30 μM) for 6 h or with 5-FU (100 and 200 μg/ml). NP-40 (1%) extracted DNA was purified and run on 2% agarose gel. M indicates 100 bp DNA ladder of size marker. **c** TMK-1 and TMK-1-6-16 cells were treated with CHX (10 and 30 μM) for 6 h or with 5-FU (80 μg/ml) for 24 h. Cells were collected and were measured for caspase-3 activity by PhiPhilux G1D2 Kit by using Flow cytometry. Cells with FL-1H amp gain over 180 were referred to as caspase-3 positive cells

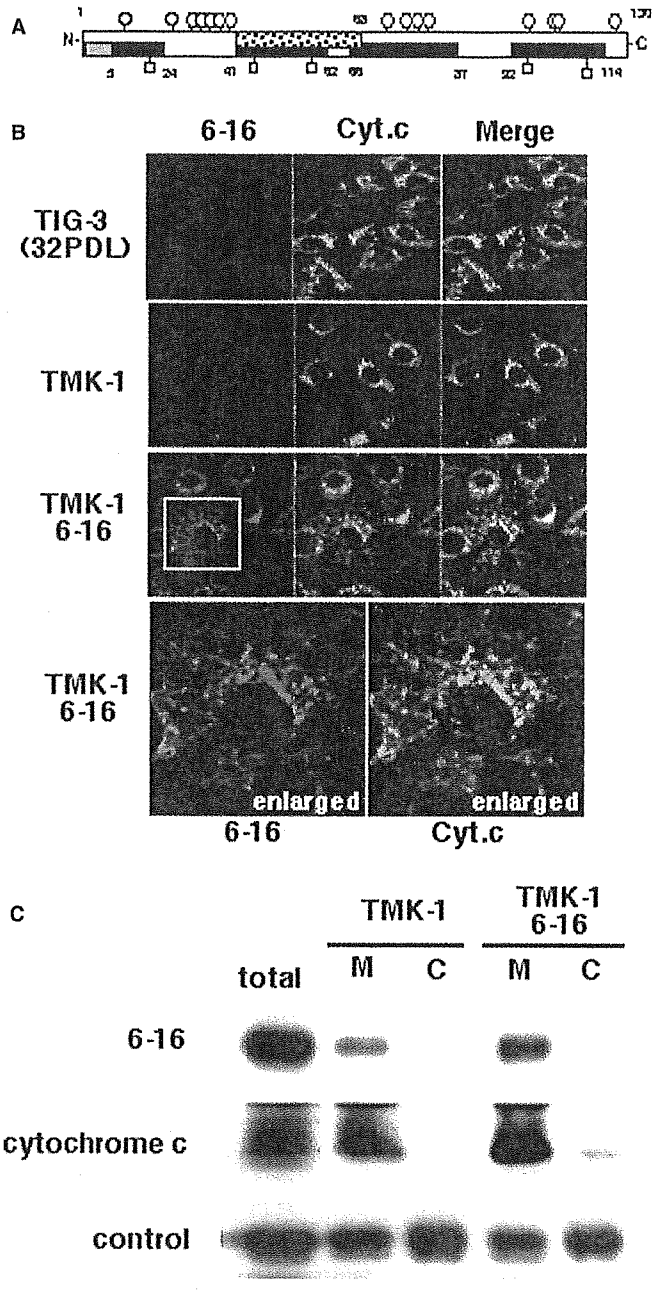

Fig. 4 6-16 co-localized with cytochrome c at mitochondria. **a** 6-16 protein has possible glycosylation sites (15 serine residues and 5 threonine residues) and possible mitochondria localization site [one intramitochondrial target sequence, one APOLAR (apolar signal of intramitochondria sorting) signal domain and four mitochondrial helices domains]. *Open circle* serine residues, *square* threonine residues, *black bar* transmembrane helices domain, *gray bar* intramitochondrial target sequence, *dotted bar* APOLAR signal domain. **b** TIG-3 (32PDLs), TMK-1 and TMK-1-6-16 cells were fixed with 4% paraformaldehyde, and permeabilized in 0.3% Triton-X100. 6-16 (red) and cytochrome c (green) were detected by immunofluorescence. Co-localization was seen by merged image of the green and red signals (yellow). **c** Localization of 6-16 protein was detected by immunoblot analysis of whole-cell lysates (total), mitochondria fraction (M) and cytosolic fraction (C). All fractions were adjusted to 20 μg proteins and analyzed by immunoblotting with anti-6-16 antibody or anti-cytochrome c antibody

(Fig. 3a). MCF-7 expressed 6-16 at high levels and was well known to apoptosis-resistant cancer cell line (Fig. 1b). In contrast to MCF-7, RKO that is well known to apoptosis sensitive cancer cell line expressed 6-16 at low levels (Fig. 1b). In addition, TMK-1 is most sensitive cancer cell line in gastric cancer cell line which showed in Fig. 1a (data not shown). Taken together, there is good correlation between 6-16 expression levels and resistance of apoptosis. The amount of DNA extracted in NP-40 buffer, called DNA ladder, was increased in TMK-1 cells after CHX or 5-FU treatment, but not in TMK-1-6-16 (Fig. 3b). The extracted DNA showed a characteristic ladder found in DNA from apoptotic cells (Fig. 3b). DNA ladder formation is dose dependent manner (data not shown). These results indicate that 6-16 protein attenuates apoptosis induced by CHX or 5-FU in TMK-1 cell.

6-16 localized at mitochondria and co-localized with cytochrome-c

The PSORT II and TMpred database analysis have shown that 6-16 protein has transmembrane helices, a mitochondria targeting sequence and an intramitochondrial sorting signal(Fig. 4a). It was quite interesting that, from database analysis on amino acid sequence, 6-16 protein has four transmembrane domains, a mitochondrial targeting sequence and an intra-mitochondrial sorting signal (Fig. 4a). So, it is possible that 6-16 is localized at mitochondria. To check this possibility, we have examined subcellular localization of 6-16. These data led us to examine intracellular localization and possible role on apoptosis of 6-16 protein. By immunofluorescence, 6-16 protein was co-localized with cytochrome c in both TMK-1 and TMK1-6-16 cells (Fig. 4b). Essentially, the same results were obtained using a colon cancer cell line, RKO, and a breast cancer cell line, MCF-7 (data not shown). 6-16 protein was not detected in normal human fibroblast, TIG-3, at 32 PDL (Fig. 4b) but was weakly detected at 75 PDL (data not shown), consistent with the previous results that the expression of 6-16 mRNA increased with cellular senescence [6]. Mitochondrial localization of 6-16 protein, as well as cytochrome c, was confirmed by immunoblotting of subcellular fractionations (Fig. 4c). Taken together with these data, 6-16 is mainly localized in mitochondria and co-localized with cytochrome c.

6-16 protein inhibits cytochrome c release and reduction of mitochondrial membrane potential

To search for the mechanism of anti-apoptotic function of 6-16, we first examined caspase-3 activity. The percentage of cells positive for caspase-3 activity determined by Flow cytometry was remarkably increased in TMK-1 cells after the treatment with CHX and 5-FU

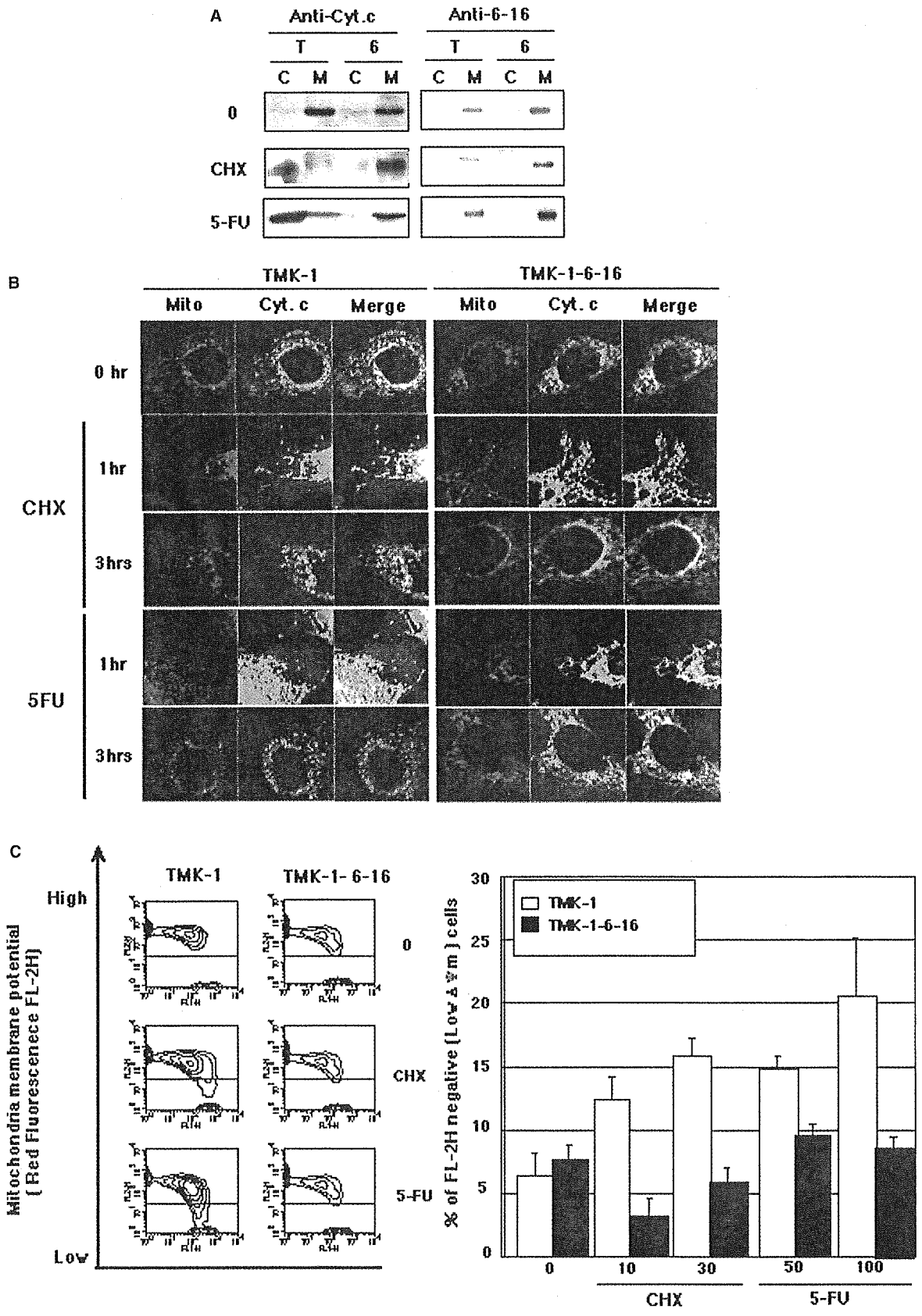
A
Anti-Cyt.c
Anti-6-16
T
6
C M C M
0
CHX
5-FU
B
TMK-1
TMK-1-6-16
Mito
Cyt. c
Merge
0 hr
1hr
3hrs
CHX
5FU
C
TMK-1
TMK-1-6-16
High
Low
Mitochondria membrane potential
(Red Fluorescenece FL-2H)
0
CHX
5-FU
% of FL-2H negative [Low Δψm] cells
0
10
30
50
100
CHX
5-FU

◀

Fig. 5 6-16 protein inhibits release of cytochrome c and reduction of mitochondrial membrane potential. **a** For immunofluorescence, cells were treated with CHX (10 μM) and 5-FU (200 μg/ml), labeled with MitoTracker CM-H_2XRos (Red) for 45 min, and fixed with 4% paraformaldehyde, permeabilized in 0.3% Triton-X100, and stained with anti-cytochrome c antibody (green). **b** TMK-1 and TMK-1-6-16 cells were treated with CHX (10 μM) for 6 h or with 5-FU (80 μg/ml) for 24 h. Cells were collected and separated to mitochondria (M) and cytosolic (C) fractions. Twenty micrograms of protein was used for immunoblot analysis with anti-cytochrome c antibody or anti-6-16 antibody. **c** TMK-1 and TMK-1-6-16 cells were treated with CHX (10 and 30 μM), 5-FU (50 and 100 μg/ml) for an hour. Cells were collected and incubated with Mitosensor reagent buffer (Clontech) for 30 min at 37°C in CO_2 incubator, and Δ Ψ m was analyzed by Flow cytometry (*left panel*). Cells with fluorescence intensity below 30 were referred to as FL-2H negative cells (*right panel*). *Error bars* represent standard deviations from three independent samples

(Fig. 3c). The increase was seen in TMK-1-6-16 only at high concentration of CHX at 30 μg/ml. These results suggested that 6-16 inhibited the caspase-3 dependent apoptotic pathway.

The apoptosis related-proteins (e.g. cytochrome c, caspase-2, −3, −9, Hsp10, Smac/DIABLO and AIF) are released from mitochondria into the cytosol during apoptosis [10, 15], and the activation of the caspase cascade is dependent on the release of cytochrome c from mitochondria [10, 16, 17]. Immunoblot analysis demonstrated that in TMK-1 cells, cytochrome c in mitochondria was released into cytosolic after treatment with CHX or 5-FU (Fig. 5a). In TMK-1-6-16 cells, however, cytochrome c was detected in mitochondria after either treatment (Fig. 5a). 6-16 protein remained in mitochondria fraction in both TMK-1 and TMK-1-6-16 cells after treatment with either CHX or 5-FU (Fig. 5a). Release of cytochrome c was also monitored by immunofluorescence staining. In non-apoptotic TMK-1 cells, the staining patterns of mitochondria (red) and cytochrome c (green) were completely overlapped (merge: yellow) (Fig. 5b). After treatment with CHX or 5-FU, the signals of cytochrome c were distinct from that of mitochondria in TMK-1 cells (Fig. 5b left panel), whereas these two signals always overlapped in TMK-1-6-16 cells (Fig. 5b right panel). When TMK-1 cells were treated with CHX or 5-FU for an hour, cytochrome c was diffusely observed in cytosol. After 3 h, cytochrome c signal appeared in granules or grains in cytosol distinct from mitochondria, indicating that cytochrome c in cytosol might interact with the protein complex including Apaf-1/pro-caspase-9 protein [16].

As the release of cytochrome c from mitochondria is well associated with depolarization of mitochondrial membrane potential (Δ Ψ m) [8–10], we next measured mitochondrial membrane potential at single cell level by Flow cytometry after staining cells with JC-1 or MitoSensor reagent [18, 19]. In TMK-1 cells, a cell population with decreased Δ Ψ m (depolarization) appeared after the treatment with CHX or 5-FU, but not in TMK-1-6-16 cells (Fig. 5c). These results overall suggested that 6-16 protein inhibits cytochrome c release from mitochondria by inhibiting depolarization of mitochondrial membrane potential (Δ Ψ m), resulting in attenuation of apoptosis.

6-16 interacts with calcium integrin binding protein, CIB

In order to further understand the anti-apoptotic mechanism of 6-16 protein, we screened 6-16 interacting protein by yeast two-hybrid methods. The fusion protein of full length 6-16 and GAL4 (GAL4-6-16) was used as bait. By the screening of 1×10^6 colonies of HeLa cDNA library, 41 positive clones (His+ and LacZ+) were identified. Among them, twenty-seven cDNA clones encoded CIB/KIP/calmyrin (we refer to it as CIB in this paper) (Genbank: U822226, U85611). CIB (calcium and integrin binding protein) [20] was also reported from independent groups as DNA-PK interaction protein (KIP) [21] and calcium-binding myristoylated protein with homology to calcineurin (calmyrin) [22]. Twelve cDNA clones encoded γ-subunit of the eukaryotic cytosolic chaperonin-containing protein, TCP-1 (CCTγ) (EMBL:X74801), one cDNA clone encoded calcium binding protein related S-100 (CAPL) protein (GenBank : M80563) and one was an unknown gene.

We next examined the association of 6-16 and CIB proteins in vitro. For this purpose, we prepared GST-tagged 6-16 protein (GST-6-16) and MBP-tagged CIB protein (MBP-CIB) by purification from *E. coli* transformed with each construct and assayed for in vitro

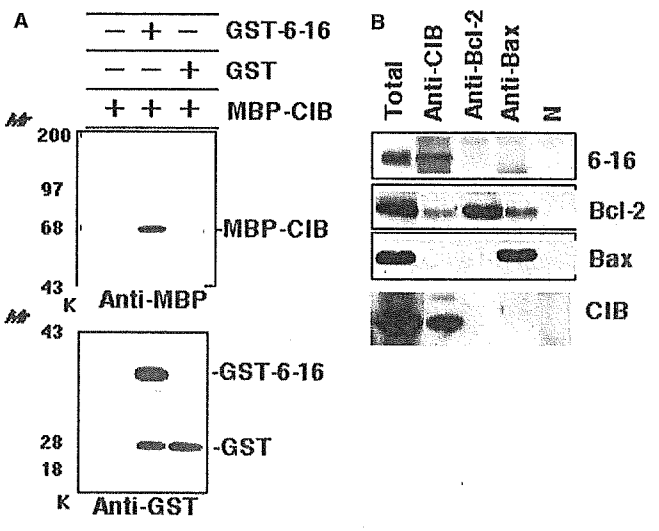

Fig. 6 CIB protein binds to 6-16 and Bcl-2 protein. **a** GST-6-16 and MBP-CIB proteins were purified from *E. coli*, and were incubated in vitro, precipitated with glutathione sepharose 4B and detected by immunoblot analysis with anti-GST antibody (*lower panel*) or anti-MBP antibody (*upper panel*). **b** MKN-28 cell extracts were immunoprecipitated with antibody against CIB, Bcl-2 or Bax (*top margin of the panel*), and subjected to immunoblot analysis with anti-6-16 antibody, anti-Bcl-2 antibody or anti-Bax antibody (*right margin of the panel*)

binding. As shown in Fig. 6a, GST-6-16 and MBP-CIB proteins co-immunoprecipitated in vitro, and 6-16 interacted with CIB using by immunoprecipitation with MKN-28 cell extracts in vivo (Fig. 6b).

We demonstrated that 6-16 protein was localized at mitochondria and attenuated apoptosis by controlling $\Delta \Psi$ m and cytochrome c release. The Bcl-2 family proteins are known to control $\Delta \Psi \mu$ and cytochrome c release via VDAC. We then hypothesized that 6-16 and/or CIB proteins might interact with Bcl-2 family proteins. For this purpose, we searched for cell lines that expressed both 6-16 and CIB at high level and found a gastric cancer cell line MKN-28, which also expressed Bcl-2 at high level (Fig. 5b). By immunoprecipitation with anti-CIB antibody, anti-Bcl-2 antibody or anti-Bax antibody followed by immunoblotting, we found that 6-16 protein interacted with CIB, but not with Bcl-2 or Bax (Fig. 6b). CIB protein interacted with 6-16 and weakly with Bcl-2, but not with Bax (Fig. 6b). Bcl-2 interacted weakly with CIB and Bax (Fig. 6b).

Discussion

In this study, we found that 6-16 protein inhibits apoptosis induced by 5-FU or CHX in gastric cancer cell line TMK-1 cells through the mitochondrial pathway. There are four different inhibition categories of apoptosis. First, in the death receptor pathway (e.g. Fas, TNF and TRAIL), RIP (receptor-interacting protein), c-FLIP (cellular-Flice-like inhibitory protein) and FAP-1 (Fas-associated phosphatese-1) inhibit death signal from the death receptors nearly located at the plasma membrane [23, 24]. Second, in the mitochondrial pathway, anti-apoptotic Bcl-2 family proteins prevent mitochondrial membrane permeabilization to inhibit mitochondrial membrane potential change and cytochrome c release [25]. Third, IAPs (inhibition of apoptosis proteins), including XIAP, cIAP-1 and cIAP-2, selectively inhibit the activity and activation of various caspases [17, 24]. Heat shock proteins (e.g. Hsp10, 27, 60, 70 and 90) also can promote or inhibit caspase activation by altering the conformation of various proteins. Finally, in degradation of chromosomal DNA during apoptosis, ICAD inhibit CAD activity as CAD/ICAD complex [26, 27]. Among these four categories, we found that 6-16 protein inhibits mitochondria-mediated apoptosis as well as anti-apoptotic Bcl-2 family proteins. BH4 domain of anti-apoptotic Bcl-2 family members closes VDAC and inhibits apoptotic mitochondrial changes and cell death [28, 29]. However, 6-16 protein does not have a BH-4 domain by protein domain homology analysis, suggesting that it may function via novel anti-apoptotic mechanisms different from Bcl-2 family proteins. It is important to understand the mechanism of up-regulation of 6-16 expression in cancer cells. Previously, we have found that 6-16 expression was up-regulated in senescent cells through beta interferon signaling pathway, because 6-16 expression was blocked by anti-INF-beta treatment to cultured senescent cells. It is possible that cancer cells may produce beta interferon and induce 6-16 expression by autocrine mechanism, but further examination are need to conclude this possibility.

Cancer and senescence may be viewed as a balance between proliferation and cell death. Many anticancer drugs are designed to induce apoptosis via cytochrome c/Apaf-1/caspase-9 (apoptosome) pathway [16, 24], and the mitochondria play a crucial role for the regulation of tumorigenesis and senescence. Apoptosis induced by CHX is mediated by the apoptosome pathway, whereas 5-FU induced apoptosis is owing to both the Fas/FasL pathway and the apoptosome pathway [24]. 5-FU treatment results in a p53-dependent increase in expression of FasL in human colon cancer cell lines, and apoptosis occurs through Fas/FasL pathway. One of the Fas/FasL pathways also acts to mitochondria after mediating BID and caspase-8. As Fas is expressed in TMK-1 cells (unpublished data), 6-16 protein also inhibits at the mitochondria the apoptosis signal via both the Fas/FasL pathway and the apoptosome pathway in gastric cancer cell line, TMK-1 cells. Therefore, because 6-16 is strongly expressed in almost all the gastrointestinal cancer cells, it is a possibly that 6-16 protein at mitochondria is involved in resistance to anticancer drugs. Free radicals, apoptosis inducers, are known to induce cellular senescence and increase with cellular senescence. 6-16 expression increased with senescence and may also inhibit apoptosis by free radical and maintain cell viability in senescence cells.

Interferon (IFN) has antiviral activity and is also known to induce apoptosis. When cells are infected with virus, 6-16 is expressed after induction of IFN. Then, an increase in 6-16 expression may cause resistance against apoptosis after viral infection. If so, IFN has apparently conflicting dual functions of both induction and inhibition of apoptosis.

We identified CIB as a 6-16 interacting protein through yeast two-hybrid screening methods. CIB protein was reported to interact with cytoplasmic domain of integrin αIIbß3 [20], eukaryotic DNA-dependent protein kinase DNA-Pkcs [21], presenilin 2 (PS2) [22], and the polo-like protein kinases Fnk and Snk [30]. The structural properties of CIB indicate that it is a hydrophilic calcium-binding protein with two EF-hand motifs corresponding to the two C-terminal Ca^{2+} binding domains, most similar to calcineurin B (58% similarity) and calmodulin (56% similarity) [20]. Calcineurin is found to dephosphorylate BAD, a pro-apoptotic member of the Bcl-2 family, thus enhancing BAD heterodimerization with Bcl-X_L and promoting apoptosis. Therefore, CIB might possess protein phosphatase activity like calcineurin or other BH3 only group of Bcl-2 family proteins to promote apoptosis. It is of interest that CIB interacts with 6-16, but further examinations are needed to conclude the involvement in the anti-apoptotic activity.

Intracellular Ca^{2+} concentration changes are important as early events in apoptosis, and maintenance of both mitochondrial and ER Ca^{2+} pool is necessary for cell survival [31, 32]. CIB (calmyrin) was found to form the complexes including presenilin, ß- and delta-catenin, p0071, amyloid ß-protein precursor, filamin/Fh-1, Notch, GSK3ß, Rab11, QM/Jif-1 and Bcl-X_L. Moreover, Presenilin 2 interacts with Sorcin, which is a penta-EF-hand Ca^{2+} -binding protein that modulates the ryanodine receptor (RyR) intracellular channel [33]. Presenilin 1 and 2 are well known for their role in Alzheimer's disease, which is associated with accumulation of ß-amyloid (amyloidogenic Aß42 peptide), abnormality of the mechanism in ER (endoplasmic reticulum) and increased rate of mitochondria-mediated apoptosis in selected areas of the brain [34]. CIB interacted with PS2, and overexpression of CIB and/or PS2 promotes cell death in vitro [22]. In fact, transfection of CIB into TMK-1 and MKN-28 cells also induced apoptosis (unpublished data). 6-16 and CIB may regulate not only mitochondria channels but also Ca^{2+} channels in ER (endoplasmic reticulum). CIB co-localizes and interacts with PS2 localized in the ER [22], and 6-16 possibly localizes at ER membrane because 6-16 has ER membrane retention signal of XXRR-like motif in the N-terminus revealed by PSORT search. Bcl-2 protein is also reported to localize not only at mitochondrial membrane but also at ER and nuclear membrane, and Bcl-2 modulates both mitochondrial and ER Ca^{2+} concentration [31, 32].

Our results indicate that 6-16 and CIB may play a critical role in the regulation of apoptosis via controlling mitochondrial and ER channels through the interaction with Bcl-2 family proteins. Therefore, 6-16 may function as a cell survival protein and CIB as cell death protein. Further examination is needed for understanding the function of interaction of 6-16 protein and CIB protein. However, these data provide a new mechanism in protecting apoptosis. It is possible that the IFN-inducible gene, 6-16 is a new target for cancer therapy and mitochondrial diseases.

Acknowledgements Yeast L-40 strain and pBTM116/HA for yeast two-hybrid screening were kindly supplied by Dr Y Takai (Osaka University, Japan). Anti-GST rabbit pAb was kindly provided by Dr. M. Nakata (Sumitomo Electric Industries, Japan). Anti-human CIB/KIP/calmyrin antibody was kindly provided by Leslie V. Parise (North Carolina University, USA). A mammalian expression plasmid, pCXN was kindly provided by Dr J. Miyazaki (Osaka University, Japan). This work was supported by Grant-in Aid from the Ministry of Education, Science, Sports and Culture of Japan.

References

1. Kelly JM, Porter AC, Chernajovsky Y, Gilbert CS, Stark GR, Kerr IM (1986) Characterization of a human gene inducible by alpha- and beta- interferons and its expression in mouse cells. Embo J 5: 1601
2. Itzhaki JE, Barnett MA, MacCarthy AB, Buckle VJ, Brown WR, Porter AC (1992) Targeted breakage of a human chromosome mediated by cloned human telomeric DNA. Nat Genet 2: 283
3. Turri MG, Cuin KA, Porter AC (1995) Characterisation of a novel minisatellite that provides multiple splice donor sites in an interferon-induced transcript. Nucleic Acids Res 23: 1854
4. Porter AC, Chernajovsky Y, Dale TC, Gilbert CS, Stark GR, Kerr IM (1988) Interferon response element of the human gene 6-16. Embo J 7: 85
5. Tahara H, Hara E, Tsuyama N, Oda K, Ide T (1994) Preparation of a subtractive cDNA library enriched in cDNAs which expressed at a high level in cultured senescent human fibroblasts. Biochem Biophys Res Commun 199: 1108
6. Tahara H, Kamada K, Sato E, Tsuyama N, Kim JK, Hara E, Oda K, Ide T (1995) Increase in expression levels of interferon-inducible genes in senescent human diploid fibroblasts and in SV40-transformed human fibroblasts with extended lifespan. Oncogene 11: 1125
7. Rao L, Debbas M, Sabbatini P, Hockenbery D, Korsmeyer S, White E (1992) The adenovirus E1A proteins induce apoptosis, which is inhibited by the E1B 19-kDa and Bcl-2 proteins. Proc Natl Acad Sci U S A 89: 7742
8. De Laurenzi V, Melino G (2000) Apoptosis. The little devil of death. Nature 406: 135
9. Capaldi RA (2000) The changing face of mitochondrial research. Trends Biochem Sci 25: 212
10. Loeffler M, Kroemer G (2000) The mitochondrion in cell death control: certainties and incognita. Exp Cell Res 256: 19
11. Antonsson B, Martinou JC (2000) The Bcl-2 protein family. Exp Cell Res 256: 50
12. Nakayama J, Tahara H, Tahara E, Saito M, Ito K, Nakamura H, Nakanishi T, Ide T, Ishikawa F (1998) Telomerase activation by hTRT in human normal fibroblasts and hepatocellular carcinomas. Nat Genet 18: 65
13. Radinsky R, Bucana CD, Ellis LM, Sanchez R, Cleary KR, Brigati DJ, Fidler IJ (1993) A rapid colorimetric in situ messenger RNA hybridization technique for analysis of epidermal growth factor receptor in paraffin-embedded surgical specimens of human colon carcinomas. Cancer Res 53: 937
14. Yokozaki H (2000) Molecular characteristics of eight gastric cancer cell lines established in Japan. Pathol Int 50: 767
15. Hengartner MO (2000) The biochemistry of apoptosis. Nature 407: 770
16. Li P, Nijhawan D, Budihardjo I, Srinivasula SM, Ahmad M, Alnemri ES, Wang X (1997) Cytochrome c and dATP-dependent formation of Apaf-1/caspase-9 complex initiates an apoptotic protease cascade. Cell 91: 479
17. Bratton SB, MacFarlane M, Cain K, Cohen GM (2000) Protein complexes activate distinct caspase cascades in death receptor and stress-induced apoptosis. Exp Cell Res 256: 27
18. Cossarizza A, Baccarani-Contri M, Kalashnikova G, Franceschi C (1993) A new method for the cytofluorimetric analysis of mitochondrial membrane potential using the J-aggregate forming lipophilic cation 5,5′,6,6′-tetrachloro-1,1′,3,3′-tetraethylbenzimidazolcarbocyanine iodide (JC-1). Biochem Biophys Res Commun 197: 40
19. Cossarizza A, Ceccarelli D, Masini A (1996) Functional heterogeneity of an isolated mitochondrial population revealed by cytofluorometric analysis at the single organelle level. Exp Cell Res 222: 84
20. Naik UP, Patel PM, Parise LV (1997) Identification of a novel calcium-binding protein that interacts with the integrin alpha-IIb cytoplasmic domain. J Biol Chem 272: 4651
21. Wu X, Lieber MR (1997) Interaction between DNA-dependent protein kinase and a novel protein KIP. Mutat Res 385: 13
22. Stabler SM, Ostrowski LL, Janicki SM, Monteiro MJ (1999) A myristoylated calcium-binding protein that preferentially interacts with the Alzheimer's disease presenilin 2 protein. J Cell Biol 145: 1277
23. Desagher S, Martinou JC (2000) Mitochondria as the central control point of apoptosis. Trends Cell Biol 10: 369

24. Kaufmann SH, Earnshaw WC (2000) Induction of apoptosis by cancer chemotherapy. Exp Cell Res 256: 42
25. Vander Heiden MG, Thompson CB (1999) Bcl-2 proteins: regulators of apoptosis or of mitochondrial homeostasis? Nat Cell Biol 1: E209
26. Sakahira H, Enari M, Nagata S (1998) Cleavage of CAD inhibitor in CAD activation and DNA degradation during apoptosis. Nature 391: 96
27. Enari M, Sakahira H, Yokoyama H, Okawa K, Iwamatsu A, Nagata S (1998) A caspase-activated DNase that degrades DNA during apoptosis, its inhibitor ICAD. Nature 391: 43
28. Shimizu S, Narita M, Tsujimoto Y (1999) Bcl-2 family proteins regulate the release of apoptogenic cytochrome c by the mitochondrial channel VDAC. Nature 399: 483
29. Shimizu S, Konishi A, Kodama T, Tsujimoto Y (2000) BH4 domain of antiapoptotic Bcl-2 family members closes voltage-dependent anion channel and inhibits apoptotic mitochondrial changes and cell death. Proc Natl Acad Sci U S A 97: 3100
30. Kauselmann G, Weiler M, Wulff P, Jessberger S, Konietzko U, Scafidi J, Staubli U, Bereiter-Hahn J, Strebhardt K, Kuhl D (1999) The polo-like protein kinases Fnk and Snk associate with a Ca(2+)- and integrin-binding protein and are regulated dynamically with synaptic plasticity. Embo J 18: 5528
31. Foyouzi-Youssefi R, Arnaudeau S, Borner C, Kelley WL, Tschopp J, Lew DP, Demaurex N, Krause KH (2000) Bcl-2 decreases the free Ca2+ concentration within the endoplasmic reticulum. Proc Natl Acad Sci U S A 97: 5723
32. Zhu L, Ling S, Yu XD, Venkatesh LK, Subramanian T, Chinnadurai G, Kuo TH (1999) Modulation of mitochondrial Ca(2+) homeostasis by Bcl-2. J Biol Chem 274: 33267
33. Pack-Chung E, Meyers MB, Pettingell WP, Moir RD, Brownawell AM, Cheng I, Tanzi RE, Kim TW (2000) Presenilin 2 interacts with sorcin, a modulator of the ryanodine receptor. J Biol Chem 275: 14440
34. Gething MJ (2000) Presenilin mutants subvert chaperone function. Nat Cell Biol 2: E21

Journal of Pathology
J Pathol 2005; **205**: 65–73
Published online in Wiley InterScience (www.interscience.wiley.com). **DOI:** 10.1002/path.1684

Original Paper

Histone H3 acetylation is associated with reduced p21$^{WAF1/CIP1}$ expression by gastric carcinoma

Yoshitsugu Mitani,[1,2] Naohide Oue,[1] Yoichi Hamai,[1] Phyu Phyu Aung,[1] Shunji Matsumura,[1] Hirofumi Nakayama,[1] Nobuyuki Kamata[2] and Wataru Yasui[1]*

[1]*Department of Molecular Pathology, Hiroshima University Graduate School of Biomedical Sciences, Hiroshima, Japan*
[2]*Department of Oral and Maxillofacial Surgery, Division of Cervico-Gnathostomatology, Hiroshima University Graduate School of Biomedical Sciences, Hiroshima, Japan*

Correspondence to: Professor Wataru Yasui, Department of Molecular Pathology, Hiroshima University Graduate School of Biomedical Sciences, 1-2-3 Kasumi, Minami-ku, Hiroshima, 734-8551, Japan. E-mail: wyasui@hiroshima-u.ac.jp

Abstract

Histone acetylation appears to play an important role in transcriptional regulation. Inactivation of chromatin by histone deacetylation is involved in the transcriptional repression of several tumour suppressor genes, including $p21^{WAF1/CIP1}$. However, the *in vivo* status of histone acetylation in human cancers, including gastric carcinoma, is not well understood. This study shows that histone H3 in the $p21^{WAF1/CIP1}$ promoter region is hypoacetylated and that this hypoacetylation is associated with reduced $p21^{WAF1/CIP1}$ expression in gastric carcinoma specimens. Chromatin immunoprecipitation assays revealed that histone H3 was hypoacetylated in the $p21^{WAF1/CIP1}$ promoter and coding regions in 10 (34.5%) and 10 (34.5%) of 29 gastric carcinoma specimens, respectively. Hypoacetylation of histone H4 in the $p21^{WAF1/CIP1}$ promoter and coding regions was observed in 6 (20.7%) and 16 (55.2%) of 29 gastric carcinoma specimens, respectively. $p21^{WAF1/CIP1}$ mRNA levels were associated with histone H3 acetylation status in the $p21^{WAF1/CIP1}$ promoter region ($p = 0.047$) but not $p53$ mutation status ($p = 0.460$). In gastric carcinoma cell lines, expression of p21$^{WAF1/CIP1}$ protein was induced by trichostatin A, a histone deacetylase inhibitor. This induction was associated with hyperacetylation of histone H3 in the $p21^{WAF1/CIP1}$ promoter region. Hyperacetylation of histone H4 in the $p21^{WAF1/CIP1}$ promoter region did not appear to be associated with increased expression. Induction of p21$^{WAF1/CIP1}$ protein expression was associated with hyperacetylation of histones H3 and H4 in the $p21^{WAF1/CIP1}$ coding region. Expression of a dominant-negative mutant of p53 reduced expression of p21$^{WAF1/CIP1}$ protein. Histone H4 acetylation in both the promoter and coding regions of the $p21^{WAF1/CIP1}$ gene in cells expressing dominant-negative p53 was less than half of that in cells expressing wild-type p53, whereas histone H3 acetylation in both the promoter and coding regions was slightly reduced (by approximately 20%) in cells expressing the dominant-negative p53. These findings provide evidence that alteration of histone acetylation occurs in human cancer tissue specimens such as those from gastric carcinoma.

Received: 6 April 2004
Revised: 22 September 2004
Accepted: 26 September 2004

Keywords: histone acetylation; histone H3; histone H4; chromatin immunoprecipitation; p53; gastric carcinoma; p21$^{WAF1/CIP1}$

Introduction

A variety of genetic and epigenetic alterations are associated with gastric carcinoma (GC) [1,2]. We have reported reduced expression of p21$^{WAF1/CIP1}$ in 34% of GC tissues [3]. $p21^{WAF1/CIP1}$ was identified through its activation by p53 [4], association with cyclin/cyclin-dependent kinase complexes [5], and increased expression during senescence [6]. Although p21$^{WAF1/CIP1}$ is activated in a p53-dependent manner in response to DNA damage to ensure cell-cycle arrest and DNA repair, various agents that promote differentiation can increase p21$^{WAF1/CIP1}$ expression in a p53-independent manner. We have also reported that p21$^{WAF1/CIP1}$ expression is induced by 9-*cis*-retinoic acid [7] and inhibition of telomerase [8], but we found no correlation between expression of p21$^{WAF1/CIP1}$ and abnormal accumulation of p53 in GC tissues [3].

Changes in DNA methylation patterns, such as hypermethylation of CpG islands, are observed frequently in human cancers [9]. Hypermethylation of CpG islands in promoters is associated with the silencing of some tumour suppressor genes [10]. Methylation and inactivation of various genes have been reported in GC [11,12]. Although hypermethylation of the $p21^{WAF1/CIP1}$ promoter occurs in acute lymphoblastic leukaemia [13], the $p21^{WAF1/CIP1}$ promoter is not hypermethylated in GC [14].

Several lines of evidence suggest that histone acetylation plays an important role in transcriptional

regulation [15]. There appears to be a positive correlation between the level of histone acetylation at specific loci and transcriptional activity, and the recruitment of histone acetyltransferases and hyperacetylation of histones in promoter regions often correlate with transcriptional activation [16,17]. Histone hyperacetylation is thought to relax the chromatin structure and allow transcription factors to access promoter sequences [18,19]. Some genes, including $p21^{WAF1/CIP1}$ [20] and *hTERT* [21], are thought to be regulated by histone acetylation. We have reported that trichostatin A (TSA), a histone deacetylase (HDAC) inhibitor, induces $p21^{WAF1/CIP1}$ expression in GC cell lines [22].

Taken together, the currently available data suggest that reduced expression of $p21^{WAF1/CIP1}$ in GC tissues may be due to aberrant histone acetylation and not p53. Little is known, however, about the *in vivo* histone acetylation status in human cancers, including GC. To date, there are no reports of changes in promoter acetylation in human cancer specimens. Thus, we investigated the histone acetylation status of the $p21^{WAF1/CIP1}$ promoter region by means of chromatin immunoprecipitation (ChIP) assays with antibodies against the acetylated forms of histones H3 and H4. Because a recent study in yeast suggested that hypoacetylation of histones in coding regions is important for transcriptional inhibition [23], we investigated the histone acetylation status in the coding region of $p21^{WAF1/CIP1}$. We show for the first time that histone acetylation is altered in GC tissue specimens and that this can reduce $p21^{WAF1/CIP1}$ expression in a p53-independent manner.

Materials and methods

Tissue samples

Twenty-nine GC tissue specimens from 29 patients were studied. The tissue specimens were obtained from Hiroshima University Hospital and affiliated hospitals. Tumours and corresponding non-neoplastic mucosae were removed surgically, frozen immediately in liquid nitrogen, and stored at −80 °C until use. All GCs were located in the middle third of the stomach. Tissues were embedded in OCT compound (Sakura Finetechnical Co, Ltd, Tokyo, Japan) and frozen sections were prepared. After we had confirmed microscopically that the tumour specimens consisted mainly (> 50%, on a nuclear basis) of carcinoma tissue and that non-neoplastic mucosa did not show any tumour cell invasion or significant inflammatory changes, samples from embedded tissues were used for ChIP assay, RNA extraction, and genomic DNA extraction. Histological classification of GC was performed according to the Lauren classification system [24]. Tumour staging was carried out according to the TNM stage grouping [25]. Because written informed consent was not obtained, all samples were cleared of any identifying information, for strict privacy protection, before histone acetylation status was analysed. This procedure is in accordance with the Ethical Guidelines for Human Genome/Gene Research enacted by the Japanese Government and was approved by the Ethics Review Committee of the Hiroshima University School of Medicine.

Cell culture and drug treatment

Eight cell lines derived from human GCs were used. The TMK-1 cell line was established in our laboratory from a poorly differentiated adenocarcinoma [26]. Five GC cell lines of the MKN series (MKN-1, adenosquamous cell carcinoma; MKN-7, MKN-28, and MKN-74, well-differentiated adenocarcinomas; and MKN-45, poorly differentiated adenocarcinoma) were kindly provided by Dr T Suzuki. The KATO-III and HSC-39 cell lines, which were established from signet ring cell carcinomas, were kindly provided by Dr M Sekiguchi and by Dr K Yanagihara [27], respectively. All cell lines were maintained in RPMI 1640 (Nissui Pharmaceutical Co, Ltd, Tokyo, Japan) containing 10% fetal bovine serum (FBS; BioWhittaker, Walkersville, ME, USA) in a humidified atmosphere of 5% CO_2 and 95% air at 37 °C. To analyse transcriptional activation of the $p21^{WAF1/CIP1}$ gene, MKN-28, MKN-74, and KATO-III cells were incubated for 5 days with 1 μM 5-aza-2′-deoxycytidine (Aza-dC; Sigma Chemical Co, St Louis, MO, USA) or for 24 h with 300 nM TSA (Wako, Tokyo, Japan).

Stable transfection

pCMV-p53mt135 expression vector (CLONTECH, Palo Alto, CA, USA) was transfected into MKN-74 cells with FuGENE6 (Roche Diagnostics, Mannheim, Germany). pCMV-p53mt135 expresses a dominant-negative mutant of p53. The *p53* and *p53mt135* genes differ by a G-to-A transition at nucleotide 1017. Stable transfectants were selected with 2 weeks of culture with 80 μg/ml G418 (Invitrogen Corp, Carlsbad, CA, USA). Clone number 5 expressed $p21^{WAF1/CIP1}$ protein at a level lower than that of the mock transfectant (see the Results section) and was used for further analyses of the dominant-negative mutant.

ChIP assay

The ChIP assay was performed as described previously [28]. Polymerase chain reaction (PCR) analysis of immunoprecipitated DNA was performed using primers specific for the 5′ upstream region of the *ACTB* gene. PCR product (15 μl) was loaded onto 8% non-denaturing polyacrylamide gels, separated by electrophoresis, stained with ethidium bromide, and visualized under UV light to confirm that there was no genomic DNA contamination of the no-antibody control. Quantitative PCR analysis of immunoprecipitated DNAs was performed by real-time PCR. The position

Table 1. Primer sequences for RT-PCR and ChIP

Primer sequence	Annealing temperature (°C)	Product size (bp)
Quantitative RT-PCR (*p21$^{WAF1/CIP1}$*)		
F: 5′-TGGAGACTCTCAGGGTCGAAA-3′	55	87
R: 5′-GGCGTTTGGAGTGGTAGAAATC-3′		
Quantitative RT-PCR (*ACTB*)		
F: 5′-TCACCGAGCGCGGCT-3′	55	60
R: 5′-TAATGTCACGCACGATTTCCC-3′		
ChIP-PCR (*p21$^{WAF1/CIP1}$* promoter region)		
F: 5′-GGGGCTTTTCTGGAAATTGC-3′	55	116
R: 5′-CTGGCAGGCAAGGATTTACC-3′		
ChIP-PCR (*p21$^{WAF1/CIP1}$* coding region)		
F: 5′-CGCTAATGGCGGGCTG-3′	55	60
R: 5′-CGGTGACAAAGTCGAAGTTCC-3′		
ChIP-PCR (*ACTB* 5′ upstream region)		
F: 5′-CCCACCCGGTCTTGTGTG-3′	55	72
R: 5′-GGGAAGACCCTGTCCTTGTCA-3′		

and sequences of primers, and annealing temperatures, are shown in Table 1 and Figure 1A. PCR was performed with the SYBR Green PCR Core Reagents Kit (Applied Biosystems, Tokyo, Japan). Real-time detection of the emission intensity of SYBR Green bound to double-stranded DNAs was done with the ABI PRISM 7700 Sequence Detection System (Applied Biosystems). The relative histone acetylation level was determined from the threshold cycles for the promoter or coding region of the *p21$^{WAF1/CIP1}$* gene and the 5′ region of the *ACTB* gene. Reference samples (genomic DNA from MKN-1 cells) were included on each assay plate to verify plate-to-plate consistency. Plates were normalized to each other with these reference samples. The PCR amplification was performed in 96-well optical trays with caps according to the manufacturer's instructions. Quantitative PCRs were performed in triplicate for each sample primer set, and the mean of the three experiments was calculated as the relative quantification value. At the end of 40 PCR cycles, reaction products were separated electrophoretically on 8% non-denaturing polyacrylamide gels for visual confirmation of PCR products.

Quantitative reverse transcription (RT)-PCR analysis of GC tissues

Total RNA was extracted with an RNeasy Mini Kit (QIAGEN, Hilden, Germany), and 1 μg of total RNA was converted to cDNA with a First Strand cDNA Synthesis Kit (Amersham Pharmacia Biotech, Uppsala, Sweden). To analyse expression of the *p21$^{WAF1/CIP1}$* gene in GC tissue specimens, real-time RT-PCR was performed as described previously [29]. Primer sequences and annealing temperatures are shown in Table 1. PCR was performed with the SYBR Green PCR Core Reagents Kit (Applied Biosystems). Reference samples (MKN-1) were included on each assay plate to verify plate-to-plate consistency.

Western blot analysis of GC cell lines

Preparation of whole cell lysates from GC cell lines and western blotting were performed as described previously [30]. Protein concentrations were determined by Bradford protein assay (Bio-Rad, Hercules, CA, USA) with bovine serum albumin (BSA) used as the standard. Lysates (20 μg) were solubilized in Laemmli's sample buffer by boiling and then subjected to 10% SDS-PAGE followed by electrotransfer onto a nitrocellulose filter. Anti-p21$^{WAF1/CIP1}$ monoclonal antibody was purchased from PharMingen (San Diego, CA, USA). Peroxidase-conjugated anti-mouse IgG was used in the secondary reaction. The immunocomplex was visualized with an ECL Western Blot Detection System (Amersham Pharmacia Biotech). The quality and amount of each protein sample on the gel were confirmed by detection with anti-beta-actin antibody (Sigma). Autoradiographic signal intensities of the p21$^{WAF1/CIP1}$ bands on western blots were determined by densitometric scanning and normalization of these signals to those of the internal control (beta-actin).

DNA extraction and p53 mutation analysis

To examine mutations in the *p53* gene, genomic DNAs were extracted from GC specimens with a genomic DNA purification kit (Promega, Madison, WI, USA). Exons 5–8 of the *p53* gene were amplified by PCR with ten sets of primers as described previously [31]. The PCR products were purified and sequenced directly with the ABI Prism Dye Terminator Cycle Sequencing Kit (Applied Biosystems) and an ABI Prism 310 DNA Sequencer (Applied Biosystems).

Statistical methods

Differences were analysed statistically by Fisher's exact and Mann–Whitney *U*-tests. *p* values less than 0.05 were considered statistically significant.

Results

Histone acetylation status in GC tissues

To examine the *in vivo* status of histone acetylation and expression of $p21^{WAF1/CIP1}$, $p21^{WAF1/CIP1}$ mRNA levels were measured by quantitative RT-PCR (Figure 1B) and acetylation of histones H3 and H4 by ChIP in 29 GC specimens (Figure 1C). The ratio of histone acetylation levels in GC specimens relative to those in non-neoplastic mucosae (T/N) was calculated. A T/N of less than 0.5 was considered to represent hypoacetylation, and a T/N of greater than 2.0 was considered to represent hyperacetylation. Hypoacetylation of histone H3 in the promoter

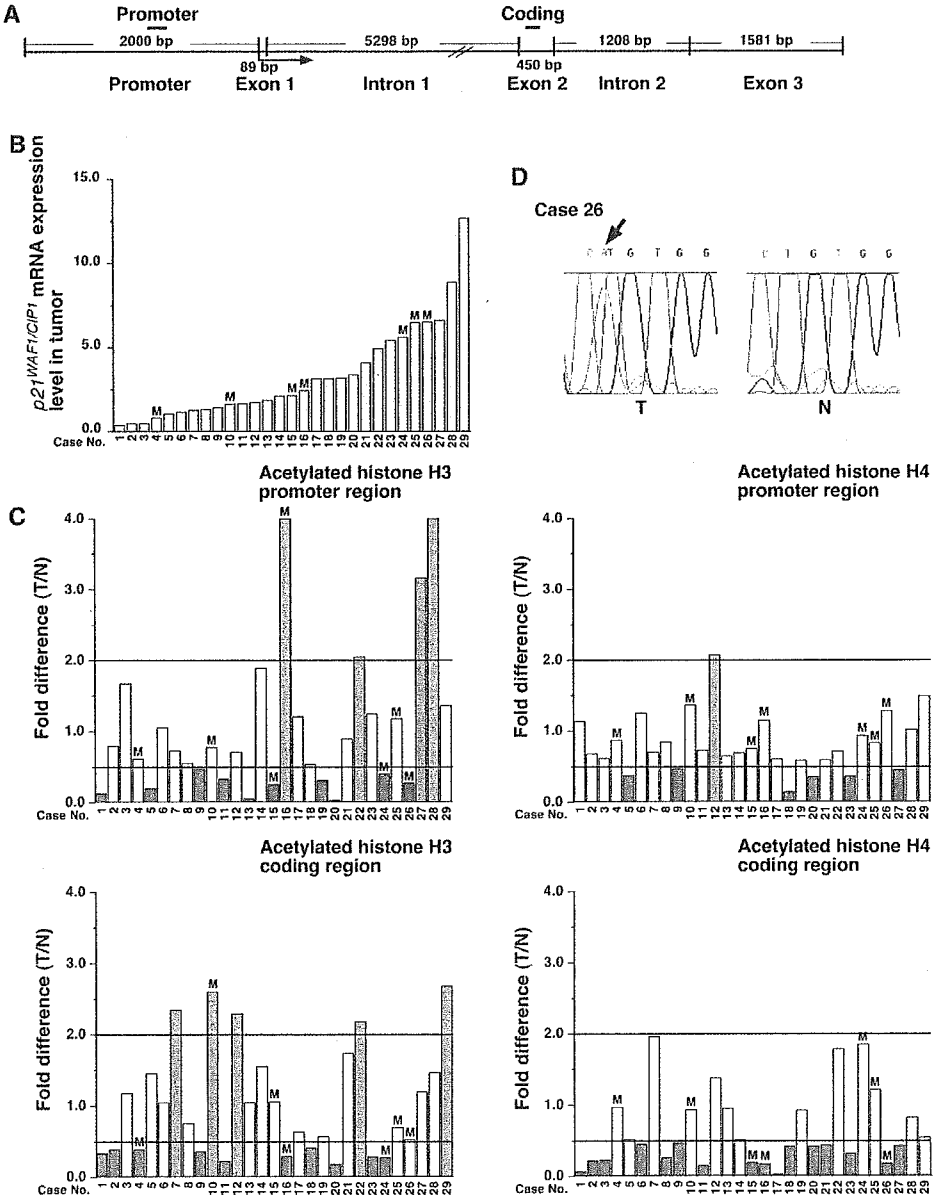

Figure 1. Expression and acetylation of the $p21^{WAF1/CIP1}$ gene and p53 mutation status in GC tissues. (A) Schematic representation of the human $p21^{WAF1/CIP1}$ gene. Positions of the primer pairs used in the present study are indicated as black bars (Promoter and Coding). (B) Quantitative RT-PCR analysis of $p21^{WAF1/CIP1}$. Units are arbitrary and we calculated $p21^{WAF1/CIP1}$ mRNA levels by standardization against 1 μg of total RNA from MKN-1 cells, which was taken as 1.0. The 29 GC tissues are sorted by increasing $p21^{WAF1/CIP1}$ expression. M indicates specimens carrying p53 mutations. (C) ChIP analysis of histones H3 and H4 in the $p21^{WAF1/CIP1}$ promoter and coding regions in 29 GC tissues. Fold change indicates the ratio of $p21^{WAF1/CIP1}$ acetylation level in GC to that in corresponding non-neoplastic mucosa (T/N). We considered a T/N < 0.5 (red bars) to indicate hypoacetylation and a T/N > 2.0 (green bars) to indicate hyperacetylation. (D) Sequencing analysis of the p53 gene (case 26, exon 5). There is a mutation in codon 145 (CTG to CAG, arrow)

and coding regions of $p21^{WAF1/CIP1}$ was observed in 10 (34.5%) and 10 (34.5%) of 29 specimens, respectively. Hypoacetylation of histone H4 in the promoter and coding regions was found in 6 (20.7%) and 16 (55.2%) of 29 specimens, respectively. $p21^{WAF1/CIP1}$ mRNA levels in tumour tissues with histone H3 hypoacetylation in the promoter region were significantly lower than those in specimens with histone H3 hyperacetylation ($p = 0.047$; Mann–Whitney U-test), whereas $p21^{WAF1/CIP1}$ levels in tumour tissues were not associated with histone H3 acetylation status in the coding region ($p = 0.540$; Mann–Whitney U-test, Table 2). No association was found between $p21^{WAF1/CIP1}$ levels and histone H4 acetylation status in either the promoter or the coding regions of $p21^{WAF1/CIP1}$.

The correlation was then examined between $p53$ mutation status and $p21^{WAF1/CIP1}$ mRNA expression, and histone acetylation. Representative results of $p53$ sequencing analysis are shown in Figure 1D, and the results of $p53$ mutation analyses are summarized in Table 3. $p53$ gene mutation was detected in 10 (34.5%) of 29 specimens. Of the ten mutations, seven were missense mutations and three were silent mutations. The seven missense mutations were analysed further. The level of $p21^{WAF1/CIP1}$ expression was not associated with $p53$ mutation status ($p = 0.460$; Mann–Whitney U-test), and $p53$ mutation status did not correlate with histone acetylation status (data not shown). Histone acetylation status was not associated with T grade (depth of tumour invasion), N grade (degree of lymph node metastasis), tumour stage, or histological type (data not shown).

TSA induced p21$^{WAF1/CIP1}$ expression and histone H3 hyperacetylation

To confirm the correlation between reduced $p21^{WAF1/CIP1}$ expression and hypoacetylation of histones, $p21^{WAF1/CIP1}$ expression and histone acetylation status were examined in eight GC cell lines. Levels of p21$^{WAF1/CIP1}$ protein were measured by western blot analysis (Figure 2A). Levels of p21$^{WAF1/CIP1}$ in GC cell lines were classified into three groups. MKN-45 and MKN-74 showed high levels of expression; MKN-28, TMK-1, and HSC-39 showed intermediate expression; and MKN-1, MKN-7, and KATO-III showed low expression. One cell line was selected from each group (MKN-74, MKN-28, and KATO-III) for further analysis. The effects of TSA and Aza-dC on p21$^{WAF1/CIP1}$ protein expression were examined by western blot analysis (Figure 2B). MKN-28 (mutant-type p53), MKN-74 (wild-type p53), and KATO-III (p53 null) cells were cultured with or without TSA for 24 h or Aza-dC for 5 days. Treatment with TSA increased the p21$^{WAF1/CIP1}$ protein levels in all three cell lines, whereas the p53 protein levels did not change. TSA induced 5.2-fold and 6.1-fold increases in p21$^{WAF1/CIP1}$ protein levels in MKN-28 and KATO-III cells, respectively, whereas TSA yielded only a 1.4-fold increase in p21$^{WAF1/CIP1}$ protein levels in MKN-74 cells. Treatment with Aza-dC had no effect on p21$^{WAF1/CIP1}$ protein expression in any of the cell lines (Figure 2B). ChIP assay was carried out to investigate acetylation of histones H3 and H4 associated with the $p21^{WAF1/CIP1}$ gene (Figure 2C). TSA increased acetylation of histone H3 in both the promoter and coding regions of $p21^{WAF1/CIP1}$ in both MKN-28 and KATO-III cells. Histone H4 acetylation in the $p21^{WAF1/CIP1}$ promoter region in MKN-28 cells was increased slightly in response to TSA, whereas that in KATO-III cells was increased significantly. Histone H4 acetylation in the coding region was increased markedly by TSA in both MKN-28 and KATO-III

Table 3. Summary of $p53$ mutations

Case No	Location	Codon	Sequence change	Amino acid
4	Exon 7	245	GGC to GTC	Gly to Val
5	Exon 5a	129	GCC to GCT	Ala to Ala
10	Exon 5b	160	ATG to ATA	Met to Ile
15	Exon 7	251	ATC to AAC	Ile to Asn
16	Exon 5b	160	ATG to ACG	Met to Thr
18	Exon 5a	129	GCC to GCT	Ala to Ala
21	Exon 7	240	AGT to AGC	Ser to Ser
24	Exon 5b	173	GTG to GCG	Val to Ala
25	Exon 5a	128	CCT to ACT	Pro to Thr
26	Exon 5a	145	CTG to CAG	Leu to Gln

Table 2. Association between $p21^{WAF1/CIP1}$ mRNA levels and histone acetylation status

		No of cases	$p21^{WAF1/CIP1}$ mRNA level (mean ± SE)*	p value†
Histone H3 acetylation status in promoter region	Hypo	10	2.71 ± 0.62	0.047
	Hyper	4	5.71 ± 1.36	
Histone H3 acetylation status in coding region	Hypo	10	2.47 ± 0.60	0.540
	Hyper	5	4.43 ± 2.16	
Histone H4 acetylation status in promoter region	Hypo	6	3.50 ± 0.89	0.617
	Hyper	1	1.71	
Histone H4 acetylation status in coding region	Hypo	16	2.73 ± 0.511	—
	Hyper	0	—	

* The units are arbitrary and we calculated the $p21^{WAF1/CIP}$ mRNA expression level by standardization against 1 μg of total RNA from MKN-1 GC cells taken as 1.0. SE = standard error.
† Mann–Whitney U-test. Hypo = hypoacetylation; Hyper = hyperacetylation.

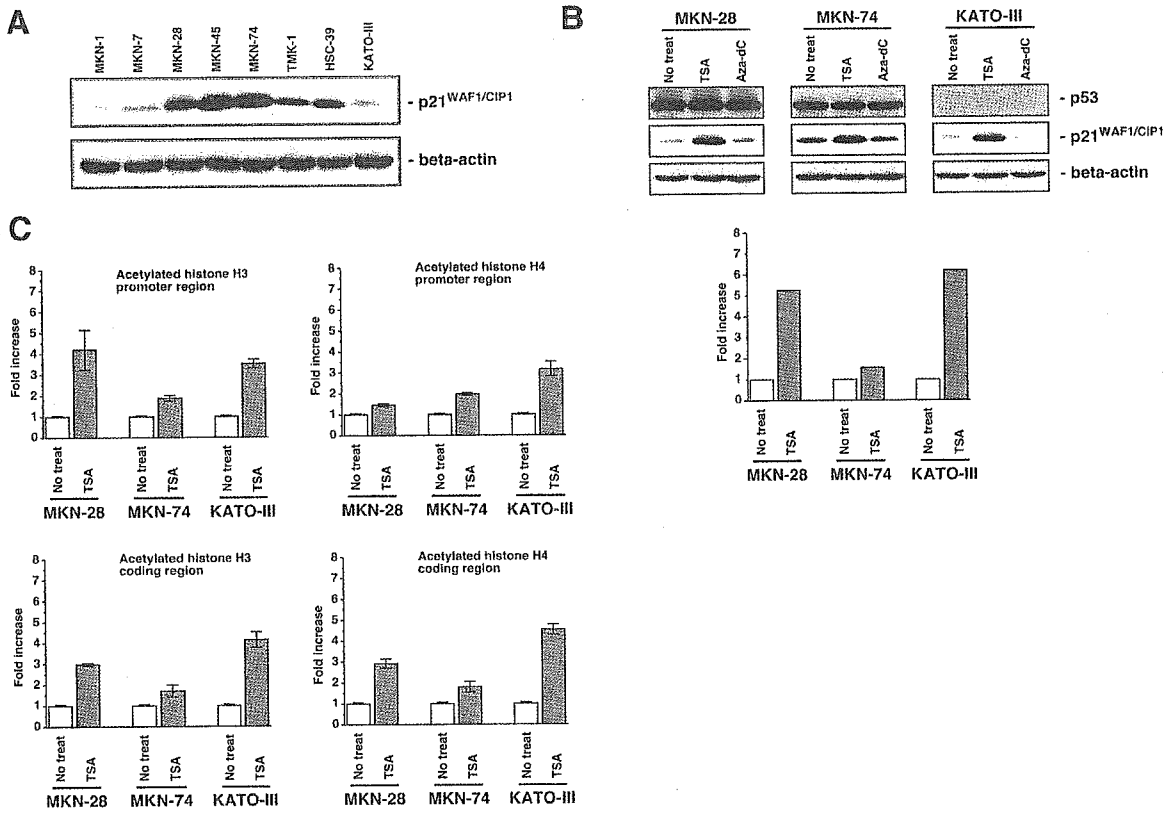

Figure 2. p21$^{WAF1/CIP1}$ protein expression and histone acetylation status in GC cell lines. (A) Western blot analysis of p21$^{WAF1/CIP1}$ in eight GC cell lines. MKN-45 and MKN-74 cells showed high expression. MKN-28, TMK-1, and HSC-39 cells showed intermediate expression. MKN-1, MKN-7, and KATO-III cells showed low expression. (B) Western blot analysis of p53 and p21$^{WAF1/CIP1}$ in three GC cell lines cultured with or without TSA for 24 h or Aza-dC for 5 days. In all three cell lines, TSA treatment induced p21$^{WAF1/CIP1}$ expression, whereas Aza-dC treatment did not. The relative p21$^{WAF1/CIP1}$ band intensity normalized to that of beta-actin is indicated in the lower panel. (C) ChIP analyses of the relative levels of histones H3 and H4 in the $p21^{WAF1/CIP1}$ promoter and coding regions in three GC cell lines. The value is the mean of three independent ChIP experiments. Error bars indicate the standard error (SE) of the mean. Note that acetylation of histone H4 in the promoter region does not increase significantly after TSA treatment in MKN-28 cells

cells. In MKN-74 cells, acetylation of histones H3 and H4 in both the promoter and coding regions was increased approximately 2.0-fold.

Inhibition of p53-induced hypoacetylation of histone H4

To investigate the effect of p53 on p21$^{WAF1/CIP1}$ protein levels, the MKN-74 cell line was stably transfected with a vector expressing a dominant-negative mutant of p53, and p21$^{WAF1/CIP1}$ protein levels were determined by western blot analysis (Figure 3A). p21$^{WAF1/CIP1}$ levels in p53 mutant cells were less than half those in wild-type cells. ChIP was also used to analyse histone acetylation levels (Figure 3B). Histone H4 acetylation levels in both the promoter and coding regions of cells expressing dominant-negative p53 were less than half those in cells expressing wild-type p53, whereas histone H3 acetylation levels in both the promoter and coding regions were reduced slightly (approximately 20%) in cells expressing dominant-negative p53.

Discussion

A variety of genetic and epigenetic alterations are associated with GC. Histone acetylation and DNA methylation appear to play important roles in transcriptional regulation; however, little is known about changes in histone acetylation in human cancers such as GC. In the present study, we investigated the histone acetylation status in regions of the $p21^{WAF1/CIP1}$ gene in GC tissues and GC cell lines.

We found that histones H3 and H4 in both the promoter and coding regions are hypoacetylated in GC tissues. $p21^{WAF1/CIP1}$ mRNA levels are associated with histone H3 acetylation status in the promoter region, suggesting that nucleosome conformation was altered due to histone H3 hypoacetylation and that access of transcriptional regulatory proteins to chromatin might be reduced in GC tissues. It is possible that histone hypoacetylation and reduced $p21^{WAF1/CIP1}$ expression were the result of the p53 mutation because previous studies have shown an interaction between p53 and chromatin-modifying enzymes.

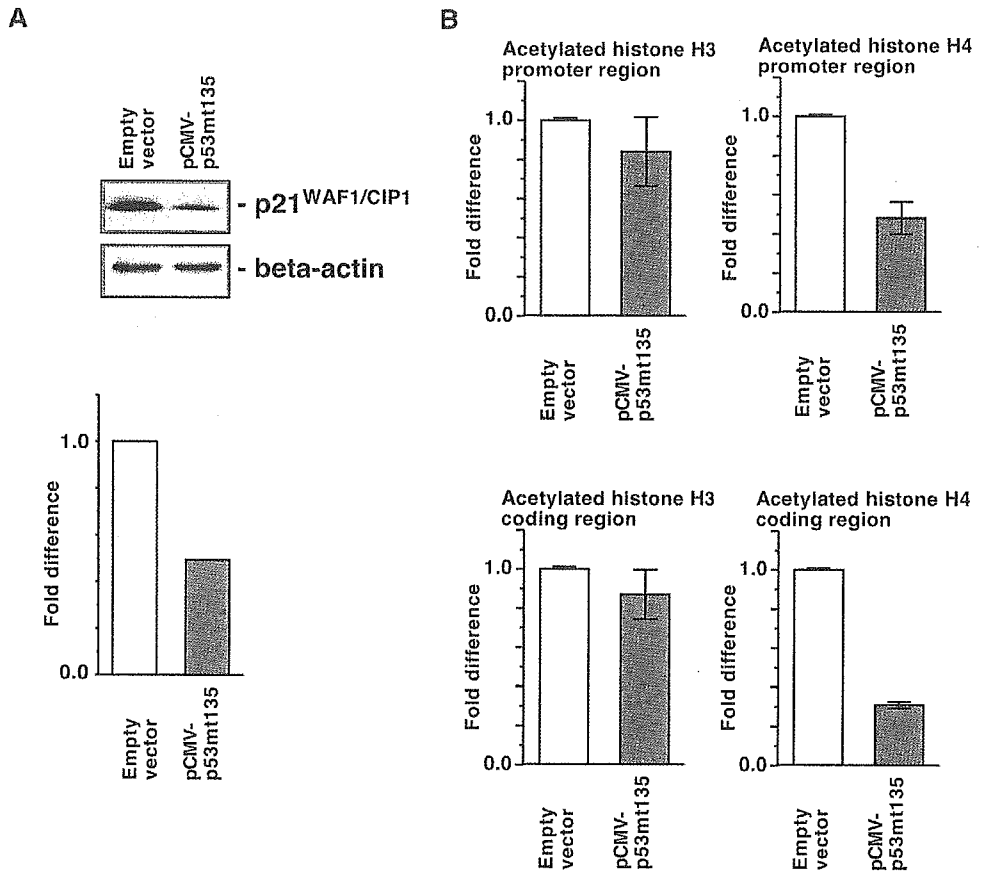

Figure 3. Effect of a dominant-negative (DN) mutant of p53 in MKN-74 cells. (A) Western blot analysis of p21$^{WAF1/CIP1}$ (upper panel). Expression of DN p53 reduced p21$^{WAF1/CIP1}$ expression. p21$^{WAF1/CIP1}$ band intensity normalized against beta-actin is indicated in the lower panel. (B) ChIP analyses of relative levels of histones H3 and H4 in the $p21^{WAF1/CIP1}$ promoter and coding regions. The value is the mean of three independent ChIP experiments. Error bars are the standard error (SE) of the mean. Note that expression of DN p53 reduced acetylation of histone H4 in both the promoter and coding regions of $p21^{WAF1/CIP1}$

Several acetyltransferases act as p53 co-activators and regulate the transcriptional activity of p53 [32,33]. In addition, we showed that a dominant-negative p53 mutant affects histone acetylation in MKN-74 cells. However, in our study, *p53* mutation status correlated with neither histone acetylation status nor $p21^{WAF1/CIP1}$ expression in GC tissues. Because several factors, such as transforming growth factor beta and nerve growth factor, have been reported to activate transcription of $p21^{WAF1/CIP1}$ [34], we cannot rule out the possibility that they cause hypoacetylation of histones in the $p21^{WAF1/CIP1}$ promoter. However, altered hypoacetylation of histone H3 in GC tissues does not appear to be due to a mutant form of p53 because p53 appears to affect acetylation of only histone H4 [35]. We also showed that expression of a dominant-negative p53 mutant suppresses p21$^{WAF1/CIP1}$ expression and that acetylation of histone H4 in the promoter is reduced significantly. Taken together, our data indicate that aberrant hypoacetylation of histones in the $p21^{WAF1/CIP1}$ promoter occurs in GC.

We found no association between $p21^{WAF1/CIP1}$ expression and histone H4 acetylation status in the $p21^{WAF1/CIP1}$ promoter in GC tissues and MKN-28 cells. In MDA-MB-435 cells, trapoxin (TPX), an HDAC inhibitor, significantly increases acetylation of histone H3 in the $p21^{WAF1/CIP1}$ promoter, whereas TPX does not significantly affect acetylation of histone H4 [36]. Similar results have been reported in HDAC1-null embryonic stem cells [37]. These results indicate that hyperacetylation of histone H4 in the $p21^{WAF1/CIP1}$ promoter region is not an absolute requirement for $p21^{WAF1/CIP1}$ expression.

HDAC inhibition appears to influence histone H3 hyperacetylation, whereas p53 appears to affect histone H4 hyperacetylation. Our present results also suggest that acetylated histones H3 and H4 have distinct roles. Distinct roles for acetylation of histones H3 and H4 have been reported in yeast [38]. Although a number of studies have shown induction of $p21^{WAF1/CIP1}$ by HDAC inhibitors, p53, and Sp1 [33,35,39], the significance of distinct roles for acetylation of histones H3 and H4 is not clear in human cancer cells. Further studies may reveal the functional significance of the acetylation of histones H3 and H4.

We also investigated the histone acetylation status in the coding region of $p21^{WAF1/CIP1}$. In GC cell lines, expression of $p21^{WAF1/CIP1}$ protein is associated with acetylation of histones H3 and H4 in the $p21^{WAF1/CIP1}$ coding region. This is consistent with the idea that transcript elongation and histone acetylation are needed to form and maintain, respectively, the relaxed structure of transcribing nucleosomes [40]. In contrast to our findings in cell lines, we found no association between $p21^{WAF1/CIP1}$ expression and histone acetylation status in the coding region in GC tissues. However, our data do show that histone H4 in the $p21^{WAF1/CIP1}$ coding region is frequently hypoacetylated in GC tissues. Although there have been many studies of promoter histone acetylation, the function of histone acetylation in coding regions is poorly understood. The significance of histone H4 hypoacetylation in the coding region of $p21^{WAF1/CIP1}$ remains unclear, but it is possible that it contributes to a change in nucleosome conformation. Further studies are needed to elucidate the function of histone acetylation in coding regions.

In conclusion, we have shown that histones H3 and H4 in both the promoter and coding regions of the $p21^{WAF1/CIP1}$ gene are frequently hypoacetylated in GC tissues. Hypoacetylation of histone H3 in the promoter region is associated with reduced expression of $p21^{WAF1/CIP1}$ in a p53-independent manner. Clinical trials of HDAC inhibitors as cancer therapeutics are underway [41,42]. Although we did not investigate the anti-tumour activity of $p21^{WAF1/CIP1}$ and HDAC inhibitors in GC, our data provide supporting evidence for the idea that inhibition of HDAC may be an effective therapy for patients with GC.

Acknowledgements

We thank Mr K Tominaga and Ms Y Kaneko for excellent technical assistance and advice. This work was carried out with the kind cooperation of the Research Center for Molecular Medicine (RCMM), Faculty of Medicine, Hiroshima University. This work was supported, in part, by Grants-in-Aid for Cancer Research from the Ministry of Education, Culture, Science, Sports, and Technology of Japan; and from the Ministry of Health, Labor, and Welfare of Japan.

References

1. Yasui W, Oue N, Ono S, Mitani Y, Ito R, Nakayama H. Histone acetylation and gastrointestinal carcinogenesis. *Ann N Y Acad Sci* 2003; **983**: 220–231.
2. Oue N, Hamai Y, Mitani Y, *et al.* Gene expression profile of gastric carcinoma: identification of genes and tags potentially involved in invasion, metastasis, and carcinogenesis by serial analysis of gene expression. *Cancer Res* 2004; **64**: 2397–2405.
3. Yasui W, Akama Y, Kuniyasu H, *et al.* Expression of cyclin-dependent kinase inhibitor p21WAF1/CIP1 in non-neoplastic mucosa and neoplasia of the stomach: relationship with p53 status and proliferative activity. *J Pathol* 1996; **180**: 122–128.
4. el-Deiry WS, Tokino T, Velculescu VE, *et al.* WAF1, a potential mediator of p53 tumor suppression. *Cell* 1993; **75**: 817–825.
5. Harper JW, Adami GR, Wei N, Keyomarsi K, Elledge SJ. The p21 Cdk-interacting protein Cip1 is a potent inhibitor of G1 cyclin-dependent kinases. *Cell* 1993; **75**: 805–816.
6. Noda A, Ning Y, Venable SF, Pereira-Smith OM, Smith JR. Cloning of senescent cell-derived inhibitors of DNA synthesis using an expression screen. *Exp Cell Res* 1994; **211**: 90–98.
7. Naka K, Yokozaki H, Domen T, *et al.* Growth inhibition of cultured human gastric cancer cells by 9-*cis*-retinoic acid with induction of cdk inhibitor Waf1/Cip1/Sdi1/p21 protein. *Differentiation* 1997; **61**: 313–320.
8. Naka K, Yokozaki H, Yasui W, Tahara H, Tahara E. Effect of antisense human telomerase RNA transfection on the growth of human gastric cancer cell lines. *Biochem Biophys Res Commun* 1999; **255**: 753–758.
9. Jones PA, Baylin SB. The fundamental role of epigenetic events in cancer. *Nature Rev Genet* 2002; **3**: 415–428.
10. Kass SU, Pruss D, Wolffe AP. How does DNA methylation repress transcription? *Trends Genet* 1997; **13**: 444–449.
11. Oue N, Motoshita J, Yokozaki H, *et al.* Distinct promoter hypermethylation of p16INK4a, CDH1, and RAR-beta in intestinal, diffuse-adherent, and diffuse-scattered type gastric carcinomas. *J Pathol* 2002; **198**: 55–59.
12. Oue N, Oshimo Y, Nakayama H, *et al.* DNA methylation of multiple genes in gastric carcinoma: association with histological type and CpG island methylator phenotype. *Cancer Sci* 2003; **94**: 901–905.
13. Roman-Gomez J, Castillejo JA, Jimenez A, *et al.* 5′ CpG island hypermethylation is associated with transcriptional silencing of the p21(CIP1/WAF1/SDI1) gene and confers poor prognosis in acute lymphoblastic leukemia. *Blood* 2002; **99**: 2291–2296.
14. Shin JY, Kim HS, Park J, Park JB, Lee JY. Mechanism for inactivation of the KIP family cyclin-dependent kinase inhibitor genes in gastric cancer cells. *Cancer Res* 2000; **60**: 262–265.
15. Grunstein M. Histone acetylation in chromatin structure and transcription. *Nature* 1997; **389**: 349–352.
16. Eberharter A, Becker PB. Histone acetylation: a switch between repressive and permissive chromatin. Second in review series on chromatin dynamics. *EMBO Rep* 2002; **3**: 224–229.
17. Urnov FD, Wolffe AP. Chromatin remodeling and transcriptional activation: the cast (in order of appearance). *Oncogene* 2001; **20**: 2991–3006.
18. Luger K, Richmond TJ. The histone tails of the nucleosome. *Curr Opin Genet Dev* 1998; **8**: 140–146.
19. Luger K, Mader AW, Richmond RK, Sargent DF, Richmond TJ. Crystal structure of the nucleosome core particle at 2.8 Å resolution. *Nature* 1997; **389**: 251–260.
20. Richon VM, Sandhoff TW, Rifkind RA, Marks PA. Histone deacetylase inhibitor selectively induces p21WAF1 expression and gene-associated histone acetylation. *Proc Natl Acad Sci U S A* 2000; **97**: 10014–10019.
21. Takakura M, Kyo S, Sowa Y, *et al.* Telomerase activation by histone deacetylase inhibitor in normal cells. *Nucleic Acids Res* 2001; **29**: 3006–3011.
22. Suzuki T, Yokozaki H, Kuniyasu H, *et al.* Effect of trichostatin A on cell growth and expression of cell cycle- and apoptosis-related molecules in human gastric and oral carcinoma cell lines. *Int J Cancer* 2000; **88**: 992–997.
23. Kristjuhan A, Walker J, Suka N, *et al.* Transcriptional inhibition of genes with severe histone h3 hypoacetylation in the coding region. *Mol Cell* 2002; **10**: 925–933.
24. Lauren P. The two histological main types of gastric carcinoma. Diffuse and so-called intestinal type carcinoma: an attempt at histological classification. *Acta Pathol Microbiol Scand* 1965; **64**: 31–49.
25. Sobin LH, Wittekind CH (eds). *TNM Classification of Malignant Tumors* (5th edn). Wiley-Liss: New York, 1997; 59–62.
26. Ochiai A, Yasui W, Tahara E. Growth-promoting effect of gastrin on human gastric carcinoma cell line TMK-1. *Jpn J Cancer Res* 1985; **76**: 1064–1071.
27. Yanagihara K, Seyama T, Tsumuraya M, Kamada N, Yokoro K. Establishment and characterization of human signet ring cell

gastric carcinoma cell lines with amplification of the c-myc oncogene. *Cancer Res* 1991; **51**: 381–386.
28. Ferreira R, Naguibneva I, Mathieu M, *et al.* Cell cycle-dependent recruitment of HDAC-1 correlates with deacetylation of histone H4 on an Rb-E2F target promoter. *EMBO Rep* 2001; **2**: 794–799.
29. Kondo T, Oue N, Yoshida K, *et al.* Expression of POT1 is associated with tumor stage and telomere length in gastric carcinoma. *Cancer Res* 2004; **64**: 523–529.
30. Yasui W, Ayhan A, Kitadai Y, *et al.* Increased expression of p34cdc2 and its kinase activity in human gastric and colonic carcinomas. *Int J Cancer* 1993; **53**: 36–41.
31. Oue N, Shigeishi H, Kuniyasu H, *et al.* Promoter hypermethylation of MGMT is associated with protein loss in gastric carcinoma. *Int J Cancer* 2001; **93**: 805–809.
32. Avantaggiati ML, Ogryzko V, Gardner K, Giordano A, Levine AS, Kelly K. Recruitment of p300/CBP in p53-dependent signal pathways. *Cell* 1997; **89**: 1175–1184.
33. Espinosa JM, Emerson BM. Transcriptional regulation by p53 through intrinsic DNA/chromatin binding and site-directed cofactor recruitment. *Mol Cell* 2001; **8**: 57–69.
34. Gartel AL, Tyner AL. Transcriptional regulation of the p21(WAF1/CIP1) gene. *Exp Cell Res* 1999; **246**: 280–289.
35. Lagger G, Doetzlhofer A, Schuettengruber B, *et al.* The tumor suppressor p53 and histone deacetylase 1 are antagonistic regulators of the cyclin-dependent kinase inhibitor p21/WAF1/CIP1 gene. *Mol Cell Biol* 2003; **23**: 2669–2679.
36. Sambucetti LC, Fischer DD, Zabludoff S, *et al.* Histone deacetylase inhibition selectively alters the activity and expression of cell cycle proteins leading to specific chromatin acetylation and antiproliferative effects. *J Biol Chem* 1999; **274**: 34 940–34 947.
37. Lagger G, O'Carroll D, Rembold M, *et al.* Essential function of histone deacetylase 1 in proliferation control and CDK inhibitor repression. *EMBO J* 2002; **21**: 2672–2681.
38. Wan JS, Mann RK, Grunstein M. Yeast histone H3 and H4 N termini function through different GAL1 regulatory elements to repress and activate transcription. *Proc Natl Acad Sci U S A* 1995; **92**: 5664–5668.
39. Sowa Y, Orita T, Hiranabe-Minamikawa S, *et al.* Histone deacetylase inhibitor activates the p21/WAF1/Cip1 gene promoter through the Sp1 sites. *Ann N Y Acad Sci* 1999; **886**: 195–199.
40. Walia H, Chen HY, Sun JM, Holth LT, Davie Jr. Histone acetylation is required to maintain the unfolded nucleosome structure associated with transcribing DNA. *J Biol Chem* 1998; **273**: 14 516–14 522.
41. Kelly WK, Richon VM, O'Connor O, *et al.* Phase I clinical trial of histone deacetylase inhibitor: suberoylanilide hydroxamic acid administered intravenously. *Clin Cancer Res* 2003; **9**: 3578–3588.
42. Carducci MA, Gilbert J, Bowling MK, *et al.* A Phase I clinical and pharmacological evaluation of sodium phenylbutyrate on a 120-h infusion schedule. *Clin Cancer Res* 2001; **7**: 3047–3055.